

1 **Title: Microbiome dynamics during the HI-SEAS IV mission, and implications for**
2 **future crewed missions beyond Earth**

3

4 **Authors:** Alexander Mahnert¹, Cyprien Verseux², Petra Schwendner³, Kaisa Koskinen^{1,4},
5 Christina Kumpitsch¹, Marcus Blohs¹, Lisa Wink¹, Daniela Brunner¹, Theodora Goessler¹,
6 Daniela Billi⁵ and Christine Moissl-Eichinger^{1,4*}

7 ¹ Interactive Microbiome Research, Diagnostic & Research Institute of Hygiene,
8 Microbiology and Environmental Medicine, Medical University of Graz, Neue
9 Stiftingtalstrasse 6, 8010 Graz, Austria

10 ² Laboratory of Applied Space Microbiology, Center of Applied Space Technology and
11 Microgravity (ZARM), University of Bremen, Am Fallturm 2, 28359 Bremen, Germany

12 ³ University of Florida, Space Life Sciences Lab, 505 Odyssey Way, Exploration Park, N.
13 Merritt Island, FL 32953, USA

14 ⁴ BioTechMed-Graz

15 ⁵ Department of Biology, University of Rome Tor Vergata, Via della Ricerca Scientifica
16 s.n.c, 00133 Rome, Italy

17

18 * corresponding author: christine.moissl-eichinger@medunigraz.at

19 Author contact details: AM (alexander.mahnert@medunigraz.at), CV
20 (cyprien.verseux@gmail.com), PS (petra.schwendner@ufl.edu), KK,
21 (kaisa.koskinen@medunigraz.at), CK (christina.kumpitsch@medunigraz.at), MB
22 (marcus.blohs@medunigraz.at), LW (lisa.wink@medunigraz.at), DBr
23 (danbrun0103@gmail.com), TG (theodora.kopun@gmail.com), DBi (billi@uniroma2.it),
24 CM-E (christine.moissl-eichinger@medunigraz.at)

25 BMC Microbiome Special Issue: Aeronautics and space microbiomes

26 <https://www.biomedcentral.com/collections/aerospacemicro>

27

28 **Abstract:**

29 Background

30 Human health is closely interconnected with its microbiome. Stable microbiomes in, on and
31 around the human body will be key for safe and successful long-term space travel. However,
32 longitudinal dynamics of microbiomes inside confined built environments are still poorly
33 understood. Herein we used the Hawaii Space Exploration Analog and Simulation IV (HI-
34 SEAS IV) mission, a one year-long isolation study, to investigate microbial transfer between
35 crew and habitat, in order to understand adverse developments which might occur in an outpost
36 on the Moon or Mars in the future.

37 Results

38 Longitudinal profiles of the 16S rRNA gene revealed significant differences in microbial
39 diversity and composition between samples of the built environment and its crew. While
40 microbial profiles from individual crew members were highly dynamic, the microbiome on
41 built environment surfaces remained more stable. Especially within the first 200 days, archaeal
42 signatures of *Methanobrevibacter* were regularly transferred between crew members, but did
43 not impact the microbiome on habitat surfaces. In contrast to a rather stable microbial diversity
44 recovered from surfaces of the habitat, microbial diversity from the crew's skin increased over
45 time. Quantitative observations based on qPCR supported observations of dissimilarity
46 between the built environment and its crew and was also used to track the propagation of
47 antimicrobial resistances in the habitat. Together with functional and phenotypic predictions,
48 quantitative and qualitative data both supported the observation of a delayed longitudinal
49 homogenization between the crew and their habitat, that was mainly caused by the hygiene
50 infrastructure.

51 Conclusions

52 The study highlights main routes of microbial transfer, interaction of its crew and origins of
53 microbial dynamics in an isolated set-up. We identified key targets of microbial monitoring,
54 and emphasize the need for defined baselines of microbiome diversity and abundance on
55 surfaces and skin. Targeted manipulation to counteract adverse developments of the
56 microbiome will be a highly important strategy to ensure safety during future space endeavors.

57

58 Keywords

59 confined built environments, isolation, HI-SEAS, skin microbiome, indoor microbiome, 16S

60 rRNA gene amplicons, qPCR, antimicrobial resistances, longitudinal, phenotype predictions

61

62 **Background**

63

64 This decade may see the beginning of a sustainable human presence on the Moon. The US
65 government stated their commitment to lead such an endeavor in the Space Policy Directive-1
66 [1] and current goals include landing a crew at the Moon's south pole by 2024, before
67 establishing a sustained presence there by 2028 [2]. Since 2015, ESA has been strongly
68 advocating its “Moon Village” concept, a large collaborative undertaking that would lead to a
69 permanent presence on the Moon [3]. In addition, the latest Council at ministerial level
70 anticipates a strong involvement of ESA in the US-led Moon program [4]. Other collaborators
71 include JAXA and CSA. While lunar exploration could greatly benefit different areas of
72 science and technology in itself [5,6], the Moon is expected to serve as a testing ground for
73 crewed missions to Mars. Reaching the red planet is also the stated goal of private spacecraft
74 companies, notably SpaceX [7] who aims for a landing as early as in the 2020s.

75 In such endeavors, microorganisms will inevitably co-travel with the crew: they are thought to
76 outnumber human cells in our bodies [8] and each individual releases millions of them every
77 hour [9]. A microbe-free crewed mission is unrealistic, unethical and undesirable, as our
78 microbiome is essential to our health [10]. Microbial communities may however pose, if
79 inadequately managed, serious threats to future missions.

80 The most obvious threats to the crew’s health are (opportunistic) pathogens. This risk is
81 exacerbated by crewmembers’ confinement and promiscuity, limited treatment options,
82 increased microbial transmission in microgravity [11], restricted hygienic practices, potentially
83 increased virulence and decreased antibiotic susceptibility of bacteria in space [11–14],
84 lowered immune responses of astronauts attributed to microgravity, radiation and stress
85 [11,12,15–17], and lack of competition to human-borne pathogens from environmental
86 microorganisms [18]. While no life-threatening infections have been reported during
87 spaceflight so far, (opportunistic) pathogens, which are part of the normal human-associated
88 microbial diversity, were detected on the International Space Station (ISS) [13,19]. However,
89 such pathogens might have caused tens of minor medical incidents—among which are urinary
90 tract, upper respiratory tract and subcutaneous skin infections—beyond Earth [11,16].

91 The threat increases when emergency returns become impossible, notably on a Mars journey,
92 which is expected to last at least 520 days [20]. Even in a relatively mild disease scenario, the

93 resulting decrease in productivity may be a significant loss given the high value of astronaut
94 working time.

95 Another threat comes from microorganisms' interference with equipment. First, some
96 microorganisms, referred to as technophiles, can colonize industrial materials and lead to
97 hardware malfunction, degradation of structural materials and corrosion of metal parts [21].
98 Technophiles were found onboard the Mir station [22,23] and onboard the ISS [13,19,24],
99 leading to damage of various systems [25,26]. Second, microbial contaminants could interfere
100 with biological life-support systems [27] — which could greatly contribute to the feasibility of
101 long-term missions on the Moon or Mars [28–30] — by harming the system-relevant organisms
102 through competition and/or toxicity or by making food products unsuitable for crew
103 consumption.

104 Finally, microorganisms brought alongside the crew could interfere with the search for life on
105 Mars [31,32]. One strategy to mitigate the risk of contamination could be to increase our
106 knowledge of, and to catalogue, the microbial communities we are carrying [33,34]: this would
107 help to discriminate between endogenous life and our microbiome in case of an ambiguous
108 discovery and to assess the risk of contaminants to adapt to some local (micro)environments.
109 While Mars's surface appears hostile even to microbial life, it cannot be excluded that some
110 extremophiles may reach niches where they could remain active [32].

111 In any case, microbial communities will be critical components of future space endeavors, with
112 a potentially large influence on mission success [35]. Their importance is reflected in space
113 agencies' efforts to characterize them onboard the ISS [13,19,24,36–40].

114 However, microbial monitoring on the ISS is constrained by logistical and funding challenges.
115 An alternative is to study microbiome nature and dynamics in similar, closed systems (such as
116 submarines and polar stations) or specific, ground-based analogues of long-term crewed
117 spaceflight [18,41]. While those analogues differ in some important aspects (e.g., gravity and
118 radiation) from spaceflight itself, they place a small, isolated crew in combinations of the
119 following: long-term confinement, high workloads, restricted waste disposal, limited hygiene
120 and/or low air or water quality. They offer the possibility to comprehensively monitor related
121 medical and psychological issues.

122 In the past, several studies on the indoor and human microbiome were conducted in settings
123 simulating missions to future facilities on the Moon or Mars, for instance: Mars500 (520 days)

124 [41,42], the Antarctic base Concordia (one year) [43], the inflatable lunar/Mars analogous
125 habitat (ILMAH) (30 days) [44] and the biological life-support testbed “Lunar Palace 1” (LP1;
126 105 days; [27]. For all these studies, individual parameters have to be critically considered due
127 to variations in methodologies, environmental conditions, activity, geographical location,
128 architectural design, baseline-diversity of microorganisms, contaminants from crew members
129 and cargo such as food and scientific equipment.

130 Another opportunity arose in 2015-2016: as part of the Hawaii Space Exploration Analog and
131 Simulation IV (HI-SEAS IV) mission, six people spent one year in isolation in a dome
132 (diameter: 11 meters) located at 2.5 km of altitude on the barren slopes of the Mauna Loa
133 volcano, primarily for NASA Behavioral Health and Performance (BHP) research [45]. Over
134 a period of 336 days, swab and wipe samples from habitat surfaces and crew skin were taken
135 in order to assess the microbial community fluctuation, as well as the interactions of surface
136 and skin microbiomes.

137 Our main hypotheses were that i) the microbiome of the HI-SEAS habitat would follow a
138 longitudinal homogenization between individual crew members, but also the surrounding built
139 environment, ii) overall microbial diversity would be depleted and iii) the microbiome would
140 resemble those of other long time experiments in isolated confined built environments (ICE)
141 on Earth and on the ISS.

142 **Methods**

143

144 **Setting of the HI-SEAS IV mission**

145 The one-year Hawaii Space Exploration Analog and Simulation IV (HI-SEAS IV) mission took
146 place from August 28th, 2015 to August 28th, 2016 [45] in the HI-SEAS habitat, an 11 meter in
147 diameter spherical shaped dome located at 2.5 km of altitude on the barren slopes of the Mauna
148 Loa volcano (Supplementary Fig. S1). Operated by the University of Hawaii, and funded by
149 NASA, this habitat served primarily for NASA Behavioral Health and Performance (BHP)
150 research. During HI-SEAS IV, six crew members (3 males and 3 females) selected for their
151 astronaut-like profile, four from the US and two from Europe (France and Germany), spent a
152 year there in conditions mimicking those of a Mars mission. Time was mostly spent on research
153 work (including outside work, wearing mock spacesuits), test subject duties, physical exercise
154 and household chores. The crew was physically isolated from other human beings for the whole
155 mission duration and communications had a high latency (20-minute delay in both directions).
156 The diet was mostly composed of dehydrated food, canned food, occasional fermented food
157 (yoghurt, bread, and cream cheese) made from rehydrated products and rare vegetables grown
158 on site.

159 Participants typically showered 1 to 3 times a week, for an average duration of 1.5 to 2 minutes
160 under running water (Heinicke et al., submitted); bodies were then washed with Equate's
161 Sensitive Skin Body Wash, and hair with Garnier Fructis' Pure Clean Clear 2in1. In-between
162 showers, participants occasionally used disinfecting wipes (mainly, Kirkland's Extra Large
163 Disinfecting Wipes). Hands were routinely washed with Dr. Bronner's 18-in-1 Hemp
164 Peppermint Pure-Castile liquid soap, and disinfected with germ's hand sanitizer.

165 A general cleaning of the habitat was performed every Sunday. Most hard surfaces were then
166 cleaned with Simple Green's cleaner, the kitchen floor with Comet's bleach-based powder, and
167 floors aside from the bathroom and kitchen were only vacuumed. Dishwashing was performed
168 by hand. Clothes were washed with Kirkland's UltraClean laundry detergent, either by hand or
169 in a washing machine.

170 Sources of voluntarily introduced microorganisms included the following. Fermented products
171 (sourdough bread, tempeh, cream cheese, kombucha, and yoghurt) were prepared using

172 commercial microbial mixes. Toilets were composting toilets, maintained with Sun-Mar's
173 Microbe Mix and Sun-Mar's compost swift. Cyanobacteria (*Anabaena* sp. PCC 7120 and
174 *Chroococcidiopsis* sp. CCMEE 029) were used for research purposes. Part of the kitchen waste
175 was processed in a bokashi composting system (purchased from Each One Teach One Farms,
176 Hawaii).

177 **Sampling**

178 Microbiome samples were taken every other week. Habitat/furniture surface samples were
179 taken with swabs at 4 different locations. Skin surface (front torso) samples were taken with
180 wipes from each crew member. In-mission sampling occurred from September 4th, 2015 to
181 August 5th, 2016, and an extra series of skin wipe samples was performed after mission
182 completion. The baseline (day 0) was defined as the day of the first sampling event.

183 The swab samples were taken from (Supplementary Fig. S2):

184 - the front part of the (composting) toilet bowl (high density plastic), in the upstairs bathroom,

185 - the kitchen floor (painted, waterproof plywood), in an area (between the fridge and another
186 piece of furniture) where dust tended to accumulate,

187 - the desk (medium density fiberboard overlaid with plastic laminate) in one of the bedrooms,
188 and

189 - one desk (medium density fiberboard overlaid with plastic laminate) in the main room.

190 For each habitat/furniture surface sample, a swab (552C regular swab; ethylene oxide
191 sterilized, Copan, Brescia, Italy) was moistened with autoclaved, deionized water (ELGA's
192 Vision 125 Deionizer). An area of 5 × 5 cm was sampled in three directions (horizontal, vertical
193 and diagonal). The swab was turned between each change in direction. The swab was then
194 broken at the predetermined breaking point and placed back into its original container. Field
195 controls were performed during each sampling session by waving the swab in the air for a few
196 seconds instead of sampling a surface.

197 Prior to samplings of skin surfaces, sterile 50-ml tubes were filled with one wipe (TX3211,
198 SterileWipe LP, Texwipe) and 10 ml of autoclaved, deionized water. Once the wipes were
199 homogeneously moistened, crewmembers sampled their own skin following oral and written

200 instructions. Briefly: they put on gloves, cleaned them with ethanol, took the wipe out of the
201 tube, put it flat on their hand, wiped their torso up and down and left and right, folded the wipe
202 over the target surface, wiped again with one of the clean sides, wiped with the other side and
203 put the wipe back into the original tube. 20 ml of water were then added to each tube before
204 storage. Field controls were performed during each sampling session by waving the wipe in the
205 air for a few seconds instead of wiping skin.

206 Swab and wipe samples were stored at -20°C after sampling, shipped to Europe in dry ice after
207 mission completion and then stored at -80°C until analysis.

208

209 **DNA extraction**

210 A total of 63 wipes were thawed at 4 °C overnight before transferring them to DNA-free bottles
211 (baked at 250 °C for 24 h) filled with PCR-grade water. The bottles were sonicated for 120 s ±
212 5 s with a maximal power of 240 W and a frequency of 40 kHz, and vortexed at maximum
213 speed for 1 min. The biomass-containing water suspension was concentrated to 200–500 µl
214 using UV sterilized Amicon filters (Amicon Ultra 15 ml, 50 K, Merck Millipore).

215 DNA was then extracted from cells suspended and concentrated from wipes, and from all
216 surface swabs plus 7 swab field controls (for a total of 111 swab samples), using Qiagen's
217 DNeasy PowerSoil Kit.

218

219 **16S rRNA gene amplicons**

220 Microbial profiles were based on amplicons targeting the V4 region of the 16S rRNA gene.
221 The common primer pair F515-R806 [46] with tags for Illumina sequencing were used to cover
222 most bacterial and some archaeal taxa (Supplementary Table S1). 25 µl of the PCR reaction
223 mix contained a final concentration of 200 mM each of forward and reverse primers (0.4 µl of
224 10 µM stock each), 0.1 µl TaKaRa ExTaq polymerase (5 U/µl, Clontech, Japan), 2 µl ExTaq
225 buffer with MgCl₂ (10x), 1.6 µl dNTP mix (2.5 mM), 2µl of template DNA and 18.5 µl PCR
226 grade water. PCR conditions were as follows: initial denaturation at 94 °C for 3 min, followed
227 by 35 cycles of denaturation at 94 °C for 45 s, annealing at 50 °C for 60 s, elongation at 72 °C
228 for 90 s and a final elongation step at 72 °C for 10 min. PCR fragments were evaluated for

229 product size and quantity by agarose gel (3%) electrophoresis at 70 V for 30 min. Libraries for
230 Illumina MiSeq sequencing were prepared by the Core Facility Molecular Biology at the Center
231 for Medical Research at the Medical University Graz, Austria and covered biological samples,
232 field blanks, extraction blanks as well as no-template controls of PCRs. For the NGS library,
233 DNA concentrations of the generated amplicons were normalized with a SequalPrep™
234 normalization plate (Invitrogen). After normalization of PCR products, each sample was
235 indexed with a unique barcode sequence using 8 cycles of indexing PCR. Indexed samples
236 were then pooled and purified by gel cuts. Finally, the library was sequenced on an Illumina
237 MiSeq instrument and the MiSeq Reagent Kit v3, 600 cycles (2 × 301 cycles).

238

239 **Statistics and Bioinformatics**

240 After sequencing, resulting fastq files were processed with Qiime2 versions 2018.6 – 2020.6
241 [47]. Demultiplexed reads were denoised with DADA2 [48] and an ASV (amplicon sequence
242 variant) feature table was created after truncating forward reads at position 200 and reverse
243 reads at position 150. Potential contaminants were identified and removed with Decontam [49]
244 and its prevalence method with default settings (method="prevalence", neg="is.neg",
245 threshold=0.5). Representative sequences were classified by a Naïve Bayes trained classifier
246 [50] based on Silva 128 [51,52] and a rooted phylogenetic tree for phylogenetic diversity
247 measures was created with Fasttree [53]. Core metrics for alpha and beta diversity (including
248 metrics for richness, evenness, diversity and distances) were calculated including phylogenetic
249 measures like UniFrac [54] at a depth of 3,000 sequences per sample. Diversity analysis
250 covered displays and statistics like rarefaction curves, principal coordinate analysis (PCoA),
251 procrustes analysis, biplots, Mantel tests [55], Kruskal-Wallis, bioenv [56], Spearman rank
252 correlations [57] or PERMANOVA. Meta-analysis of longitudinal microbial diversity inside
253 built environments was conducted in Qiita [58] and used datasets of the following publicly
254 available Qiita studies: 2192, 10423, 11740 and 12858. All selected studies targeted the V4
255 region of the 16S rRNA gene and were processed with Qiita standard workflows (trimmed to
256 150 bp, used Deblur for denoising of the ASVs and Greengenes 13_8 for closed reference
257 taxonomy assignments). Longitudinal analysis was based on the q2-longitudinal plugin
258 available in Qiime2 [59] and covered calculations of feature-volatility, linear-mixed-effects
259 modeling, pairwise-differences, pairwise-distances, Wilcoxon signed rank tests and Mann-
260 Withney U tests. Supervised classification and regression of sample metadata was conducted

261 with the q2-sample-classifier plugin [60] with settings for optimized feature-selection and
262 parameter tuning for RandomForest regression and classifications. Differential abundance and
263 composition of features was determined with balances in gneiss [61], ancom [62] and feature
264 rankings (feature differentials and loadings) available from aldex2 [63], songbird [64] and
265 deicode [65] were partly visualized in qurro [66]. Microbial contributions of different sources
266 and sinks were predicted with SourceTracker2 (<https://github.com/biota/sourcetracker2>; [67])
267 at a source and sink depth of 3,000 sequences per sample. Potential phenotypes and functions
268 were predicted with PiCrust2 (<https://github.com/gavinmdouglas/q2-picrust2>; [68]) using the
269 custom tree pipeline and BugBase [69–71]. Further statistics and visualizations were conducted
270 in R [72] using the libraries ggplot2 and streamgraph.

271

272 **Data availability**

273 All amplicon raw data is available at the European Nucleotide Archive ENA (EMBL-EBI
274 ERP118380). In addition to raw data, processed data is available in Qiita (study id 12858;
275 <https://qiita.ucsd.edu/>; [58]).

276

277 **qPCR (16S rRNA genes and resistance genes)**

278 Overall microbial load was determined by qPCR of the 16S rRNA gene. Two setups were used
279 to quantify Bacteria and Archaea separately (primer pair 331f-797r for bacteria [73] and primer
280 pair A806f-A958r for archaea, Supplementary Table S2). For each setup 10 µl of the SYBR
281 Green Supermix (Biorad) contained 5 µl of SsoAdvanced Universal qPCR Kit MM 2x, 0.3 µl
282 each of forward and reverse primers (10 µM), 3.4 µl of PCR-grade water and 1 µl of template
283 DNA. qPCR runs were then carried out on a Bio-Rad CFX96 thermocycler with the following
284 conditions: initial denaturation at 94 °C for 3 min, followed by 35 cycles of denaturation at 94
285 °C for 45 s, annealing at 54 °C for bacteria and 60 °C for archaea for 60 s, elongation at 72 °C
286 for 90 s and a final elongation step at 72 °C for 10 min. Quantifications of 16 qPCR runs relied
287 on serial dilutions of a cloned 16S rRNA gene of *Escherichia coli* and *Nitrososphaera*
288 *viennensis*, respectively for bacteria and archaea, into StrataClone vector pscA_AmpKan
289 according to manufacturer instructions. For reliable quantifications a minimum reaction
290 efficiency of 0.8 and a correlation coefficient above 0.9 as well as clean melting curves were

291 required. Counts in negative and no-template controls were subtracted from actual samples and
292 extrapolated per m². Finally, qPCR counts were displayed as volatility plots including linear
293 regressions with time.

294 In addition to quantifications of the microbial load, monitoring of antimicrobial resistances was
295 based on the following four selected resistance genes: *blaOXA* (class A beta-lactamase; [74],
296 *int1a* (class 1 integrase; [75]), *qacEΔ1* (biocide resistance gene, quaternary ammonium
297 compound-resistance; [74,76] and *tetM* (tetracycline resistance; [74,77]) (Supplementary Table
298 S3). As individual standards were not available, all quantifications were based on relative
299 proportions and serial dilutions (1:10, 1:100, 1:1000) of the genomic DNA of four cultures
300 (*Acinetobacter* sp., *Escherichia coli*, *Enterococcus* and *Pseudomonas aeruginosa*) with
301 reported presence of these resistances. qPCR runs were prepared with the STARlet pipetting
302 robot (Hamilton, Germany) for the Bio-Rad CFX384 instrument. PCR conditions were set to
303 initial denaturation at 95 °C for 10 min, followed by 40 cycles of denaturation at 95 °C for 15
304 s, annealing at 55 °C for 30 s, elongation at 72 °C for 30 s and a final elongation step at 72 °C
305 for 30 s. All 14 qPCR runs were normalized internally (according to qPCR counts of each
306 individual standard), counts from negative controls and no-template controls were subtracted
307 from actual samples and then extrapolated per m². Similarly, as done for qPCR counts of the
308 16S rRNA gene, antimicrobial resistances were also displayed as volatility plots with linear
309 regressions.

310

311 **Microbial nomenclature**

312 Throughout the manuscript we refer to the nomenclature assigned by the Silva 128 release. A
313 special case is the genus *Propionibacterium*. We are aware that skin-associated representatives
314 of this genus were renamed in recent releases of the Silva database to the genus *Cutibacterium*
315 [78]. However, despite the fact that human skin is a reasonable source for the detected
316 signatures of *Propionibacterium* / *Cutibacterium*, we decided to use the former annotated name
317 by the referenced Silva database release 128.

318

319 **Results**

320

321 **Overview of the microbiome of the built environment and its occupants**

322 Samples were taken from four representative locations (toilet bowl, kitchen floor, desk in one
323 of the bedrooms, desk in the main room) within the confined built environment and from the
324 skin (front torso) of six isolated crew members. Sampling was performed at 27 time points
325 spanning one year. Besides amplicon sequencing, all samples plus laboratory controls (n=186
326 in total) were subjected to quantitative PCR (qPCR) on the 16S rRNA gene to assess the overall
327 bacterial load, and on four representative resistance genes (*blaOXA*, *int1a*, *qacEΔ1*, *tetM*) to
328 assess the progression of microbial resistances on skin and surfaces over time.

329 Along with the samples, 16 types of metadata of environment and crew members were recorded
330 (selected numerical metadata is listed in Supplementary Table S4). The crew was composed of
331 three male and three female members (crewID A-F), with an average age of 30+/-4 and an
332 average body size of 176 cm +/-9 cm. During the isolation and confinement, hygiene practices
333 were restricted. On average, crew members showered preferentially on Saturdays, every 5.4
334 +/- 1.8 days (60.67 +/- 15.7 times) for about 1 min and 42 seconds +/- 47 seconds. However,
335 individual showering practices differed. For instance, some crew members showered shorter,
336 but more frequently and others showered longer, but only a few times during the isolation
337 period. The diet was mostly composed of dehydrated food, but the crew was allowed to bring
338 beneficial microbes into the habitat, e.g., starters for sourdough bread, tempeh, cream cheese,
339 kombucha and yoghurt. Toilets were composting toilets. Cyanobacteria (*Anabaena* sp. PCC
340 7120 and *Chroococcidiopsis* sp. CCMEE 029) were used for research purposes. Part of the
341 kitchen waste was processed in a bokashi composting system.

342 No direct or real-time contact to other humans except to crew members was allowed, and the
343 extravehicular activities foresaw donning of a mock spacesuit that prevented exposure to open
344 air and direct sunlight (described in [79]). Nine resupply events happened during the isolation
345 period (on days 15, 43, 79, 107, 148, 185, 223, 258, 303, 335). A total of 132 samples were
346 processed before and 43 samples after a resupply event. Temperature was stable over time
347 (mean temperature 18 °C +/- 1 °C). CO₂ levels were always in the recommended range for
348 indoor environments (400 - 1,000 ppm) with an average of 662 ppm +/- 62 ppm.

349 Denoising of demultiplexed amplicon data with DADA2 resulted in 10,016 unique features
350 (ASVs). In an initial step, we analyzed the processed controls (sampling blanks, process
351 controls, no-template controls), which showed significantly lower microbial diversity than
352 actual samples (pairwise Kruskal-Wallis $P = 1.8 \times 10^{-4}$; $H' \sim 5.7$ vs. 7.0 ; rarefaction depth of
353 7,850 sequences). Moreover, microbial composition differed significantly between samples
354 and controls, according to weighted UniFrac metrics (PERMANOVA $P = 0.001$). To clean the
355 dataset, contaminants were identified from processed controls with decontam [49] and
356 subsequently removed from the dataset. All subsequent analyses were performed with the
357 cleaned dataset, which contained 3,077,780 sequences (median frequency was 17,533
358 sequences per sample). According to rarefaction curves, sequencing depth was of sufficient
359 quality, as the Shannon diversity metric (H) plateaued at $\sim 2,500$ sequences.

360 Since we were interested in the characteristics of the microbiome profile of the different sample
361 groups, the dataset was divided into different surface types (crew [skin], built environment)
362 and sample locations (e.g., individual crew members and locations within the facility).

363

364 **The overall microbial diversity and composition of biotic (skin) and abiotic surfaces** 365 **differs significantly**

366 In the first step, we compared the alpha diversities (based on Shannon index) of all sample
367 types. Samples from the crew's skin showed significantly lower diversity than samples from
368 surfaces of the built environment (pairwise Kruskal-Wallis $P = 7.3 \times 10^{-16}$; mean $H' \sim 6.2$ vs.
369 7.5) (Fig. 1A). Significant differences were also detected in the diversity index of five crew
370 members (pairwise Kruskal-Wallis of crew member A and B: q-value 1.6×10^{-3} ; A and D: q-
371 value 1.3×10^{-3} ; A and F: 7.5×10^{-3} ; C and F: 2.7×10^{-2} ; Fig. 1C).

372 Notably, the microbial diversity on the crew's skin varied more (mean $H' \sim 5.0$ in samples from
373 crew member F to ~ 6.7 for crew member A) than that on abiotic surfaces (mean $H' \sim 7.2$ in
374 samples of the kitchen floor to ~ 7.6 in bedroom samples; Fig. 1B and Fig. 1C).

375 With respect to alpha diversity, the built environment surfaces showed only significant
376 differences between bedroom and kitchen floor samples (pairwise Kruskal-Wallis q-value
377 4.5×10^{-2} ; Fig. 1B), while richness was variable (Supplementary Fig. S3). Alpha diversity was

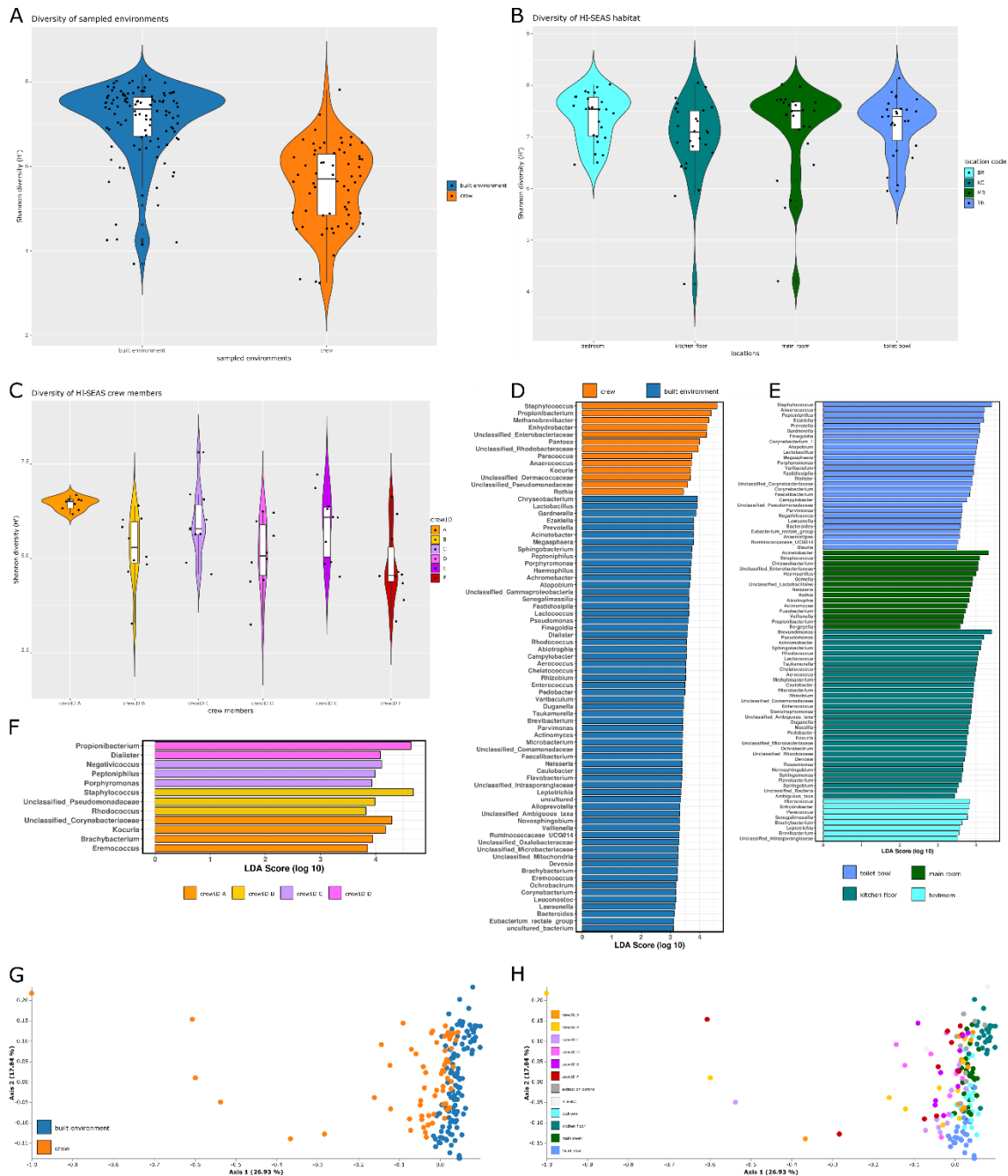
378 also significantly different according to type of surface material (plywood vs. polymer;
379 pairwise Kruskal-Wallis q-value 4.5×10^{-2} ; Supplementary Fig. S4).

380 Beyond alpha diversity, the microbiome profile of samples from built environment surfaces
381 was significantly different from that of crew skin samples (weighted UniFrac distances,
382 PERMANOVA q-value = 3×10^{-3}) and samples clustered separately in PCoA plot analysis
383 (Fig. 1G and Fig. 1H). Further significant differences were found between all four locations of
384 the HI-SEAS habitat (ranging from q-values of 1.8×10^{-3} to 3.3×10^{-3} , PERMANOVA
385 pairwise testing). However, the microbial composition was not significantly different between
386 individual crew members despite highly explained variability along PCoA Axis 1, indicating
387 dynamic changes of microbial composition on skin samples over time (see below).

388 Supported by extensive metadata analysis, the factors time ($P = 0.04$, Spearman rank
389 correlation of Shannon diversity with time) and sampling location ($P = 9.4 \times 10^{-19}$, Kruskal-
390 Wallis test of all groups, see above for more details) were identified to have a significant impact
391 on microbial diversity and the microbial profile, whereas the microclimate of the habitat
392 revealed no significant influence.

393 Metadata predictions based on Random Forest classifiers and regressors showed high overall
394 accuracy estimates of 95% for the sampling environment (skin samples vs. built environment
395 samples), and the day of sampling ($R=0.77$, $P = 2.3 \times 10^{-8}$). Thus, our subsequent analyses
396 focused on the impacts of time and sampling location.

397



398

399 **Fig. 1: Microbiome profile of crew and built environment samples, all time points included.** A to C: violin
 400 plots (kernel probability density of Shannon values, displaying the alpha diversity) including individual data
 401 points and a box with median and interquartile range. A: Sampled surface types: skin of crew and locations of the
 402 built environment. B: Built environment surfaces: BR (desk in bedroom), KC (kitchen floor), MR (desk in main
 403 room), TB (toilet bowl). C: Samples from the individual crew members (A-F). D: Linear discriminant analysis
 404 effect size (LEfSe) on samples from crew and built environment. E: LEfSe on samples from built environment
 405 surfaces. F: LEfSe on samples from individual crew members. G to H: Beta diversity represented by PCoA plots
 406 based on weighted UniFrac metrics and a rarefaction depth of 3,000 ASVs per sample. G: Microbial profile of
 407 samples from built environment and crew. H: Microbial profile of the individual crew members and sampling
 408 locations of the built environment.

409 **Each surface was characterized by a specific set of microbial signatures, which can be**
410 **predicted with high accuracy**

411 As selected surfaces of the built environment (desk in a bedroom, kitchen floor, desk in the
412 main room, toilet bowl) and the crew's skin showed a significantly different composition (see
413 below), we were interested in a detailed analysis of the characteristic features.

414 Overall, the skin samples were characterized by high abundance of *Staphylococcus*,
415 *Propionibacterium*, *Enterobacteriaceae*, *Enhydrobacter*, and *Methanobrevibacter* signatures
416 (LEfSe analysis, Fig. 1D), whereas the built surfaces were characterized by the presence of
417 *Chryseobacterium*, *Lactobacillus*, *Gardnerella*, *Prevotella*, and *Acinetobacter*.

418 Indicative microbial signatures were identified for the toilet bowl (*Staphylococcus*,
419 *Anaerococcus*), the main room desk (*Acinetobacter*, *Streptococcus*), the kitchen floor
420 (*Brevundimonas*, *Achromobacter*), and the bedroom desk surface (*Enhydrobacter*,
421 *Micrococcus*; Fig. 1E).

422 As observed for habitat surfaces, individual crew members revealed typical microbiome
423 profiles with *Propionibacterium* being indicative for crew member D, *Peptoniphilus* for crew
424 member C, *Staphylococcus* for crew member B and *Kocuria* for crew member A (Fig. 1F).
425 Remarkably, accuracy of metadata prediction based on RandomForest classifications was
426 possible for certain individuals (e.g. crew member D with 100%) or distinct surfaces of the
427 built environment (e.g. kitchen floor and the toilet bowl both 100% accuracy) (Supplementary
428 Figure S5).

429

430 **Microbial diversity on skin increased during the isolation over time**

431 Overall, the longitudinal microbial diversity in samples from skin showed a steady increase
432 over time (mean Shannon H' 4.9 to 6.4), whereas the increase in microbial diversity on built
433 environment surfaces was lower (mean Shannon H' 6.4 to 7.3). The microbial diversity from
434 built environment surfaces was subject to greater fluctuations throughout the time period (Fig.
435 2A). This observation, however, could be due to a higher number of analyzed built environment
436 samples. Increasing microbial diversity on skin was also confirmed by linear mixed effect
437 models which tested whether Shannon diversity changed over time in response to the sampling

438 locations (Supplementary Fig. S6). An increase in microbial diversity on skin was observed for
439 most crew members (C, D, E, and F; mean Shannon H' 5.1 to 6.5; highest increase for
440 individual C from 5 to 7.8). However, almost no change was visible for individual A, and a
441 slight decrease was observed for individual B (mean Shannon H' 5.5. to 4.8; Fig. 2B).

442 The microbial diversity on different locations inside the HI-SEAS habitat changed as well (Fig.
443 2B). The largest fluctuations were detected for samples of the main room, and a slight increase
444 in microbial diversity was visible for all locations apart from the toilet bowl. In the latter case,
445 microbial diversity decreased by 1 log (mean Shannon H' 7.9 to 6.8), possibly due to more
446 rigorous cleaning procedures.

447 Other metrics describing the alpha diversity of all samples, such as richness (92 to 213.67) and
448 phylogenetic diversity estimates (7.6 to 14.7), followed a similar pattern, while Pielou's
449 evenness remained constant over the entire isolation period (0.8 to 0.84; Supplementary Fig.
450 S7 and Supplementary Fig. S8).

451 Temporary dynamics of microbial diversity were investigated by pairwise difference
452 comparisons of samples from individual time points. Significant differences were only evident
453 between day 210 and day 252 for skin samples (Kruskal-Wallis test for multiple groups, $P =$
454 0.02) and between skin and built environment surface samples (Mann-Whitney U test, FDR P
455 = 0.03).

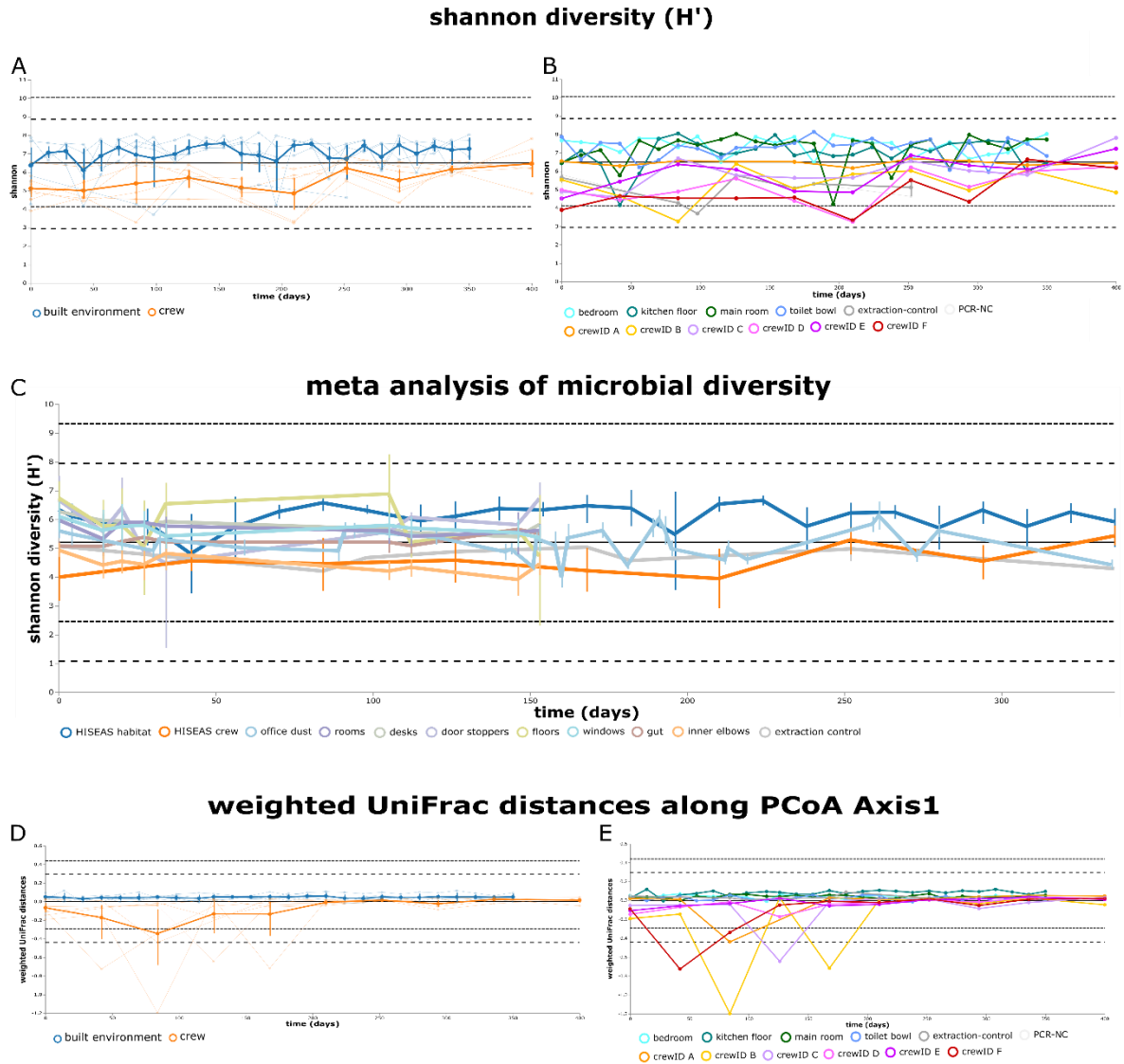
456 Furthermore, correlating patterns of microbial diversity were analyzed by Spearman rank
457 correlations. Significant positive correlations of microbial diversity were evident between crew
458 member C and D ($P = 0.05$, $\rho = 0.65$), C and E ($P = 8.8 \cdot 10^{-4}$, $\rho = 0.9$), and D and E ($P =$
459 0.02, $\rho = 0.73$). Crew member C also showed significant positive correlations of microbial
460 diversity with the kitchen floor ($P = 0.01$, $\rho = 0.82$). In contrast to these positive correlations,
461 crew member D and E showed significant negative correlations of microbial diversity with
462 samples from the bedroom surfaces ($P = 0.04$ and $P = 0.03$, $\rho = -0.7$ and $\rho = -0.75$,
463 respectively).

464 Observations of microbial composition followed a similar pattern as described for microbial
465 diversity. Hence, composition of skin samples (weighted UniFrac distances) changed to larger
466 magnitudes than those from built environment surfaces along PCoA Axis1. Largest shifts on
467 crew's skin were visible between day 0 and day 210 (with a maximum at day 84 of -0.3) (Fig.

468 2D), especially for crew member B. In contrast, almost no changes along PCoA Axis 1 were
469 visible for crew member D and E (Fig. 2E).

470 Pairwise distance comparisons of microbial composition (weighted UniFrac distances) at
471 individual time points showed significant differences between day 84 and day 126 (Kruskal-
472 Wallis test for multiple groups, $P = 0.03$), and between skin and built environment surface
473 samples (Mann-Whitney U test, FDR $P = 0.04$).

474



475

476 **Fig. 2: Longitudinal development of diversity and composition.** A: Volatility analysis of Shannon diversity
 477 resolved to sample type (built environment and human skin). B: Volatility analysis of Shannon diversity resolved
 478 to individual crew members and sampled locations within the HI-SEAS habitat. C: Meta volatility analysis of
 479 longitudinal microbial diversity of samples taken within the HI-SEAS habitat and inside other built environments.
 480 D: Volatility analysis along PCoA Axis 1 showing weighted UniFrac distances for different sample types (built
 481 environment and human skin). E: Volatility analysis along PCoA Axis 1 showing weighted UniFrac distances for
 482 individual crew members and sampled locations within the HI-SEAS habitat.

483

484 **Comparison with other built environment studies indicates an atypical increase of skin**
485 **diversity under isolation**

486 For a suitable evaluation of our observations, we performed a meta-analysis of longitudinal
487 microbial diversity patterns inside different built environments. This analysis (see Material &
488 Methods for more details) covered more than 3,400 samples and 10 different sample types
489 (front torso skin, confined habitat surfaces, office dust, room surfaces, desk surfaces, door
490 stoppers, floors, windows, fecal samples and skin samples from the inner elbow) from four
491 longitudinal studies inside the built environment. Public studies from Qiita were selected based
492 on three criteria: first they had to be longitudinal, second they had to be conducted in a built
493 environment setting and third they had to cover samples from human sources beside built
494 environment surfaces. According to these criteria we included a longitudinal analysis of
495 microbial interactions between humans and the indoor environment [80], a longitudinal
496 assessment of the influence of lifestyle homogenization on the microbiome of United States
497 Air Force Cadets [81], and a study which identified geography and location as the primary
498 drivers of office microbiome composition [82]. Our meta-analysis confirmed that microbial
499 diversity progressions in the HI-SEAS habitat were exceptional. While all other sample types
500 showed a decrease in microbial diversity, only samples from the human gut of US air force
501 cadets (mean Shannon H' 5.1 to 5.5) and skin samples of the HI-SEAS crew (mean Shannon
502 H' 4.9 to 5.4) showed a steady increase over time (Fig. 2C).

503

504 **Microbial dynamics during isolation was driven by specific taxa**

505 For a higher resolution of microbial composition over time, the isolation period was grouped
506 into four phases (phase 1: days 0 - 84, phase 2: 84 - 210, phase 3: 210 - 294 and phase 4: 294 -
507 336). To get insights into microbiome evolution after isolation, skin samples from the post-
508 mission control (day 400) were also studied.

509 According to differential abundance analysis of all samples using balances in gneiss (Fig. 3A),
510 higher proportions were visible for *Staphylococcus*, *Propionibacterium* and
511 *Methanobrevibacter* (phase 1). Between day 84 and day 210 (phase 2), only *Stenotrophomonas*
512 and unclassified Enterobacteriaceae showed higher proportions at the latter time point. Later
513 on, unclassified Dermacoccaceae, *Propionibacterium*, *Kocuria* and unclassified Rhizobiaceae
514 showed increasing proportions, while *Streptococcus* and *Fusobacterium* showed decreasing

515 proportions (phase 3). During phase 4, *Methylobacterium populi*, *Streptococcus*,
516 *Brevundimonas*, *Pseudomonas*, *Lactococcus*, *Sphingomonas* and *Cloacibacterium* revealed
517 lower proportions than unclassified Enterobacteriaceae and *Staphylococcus*.

518 After the isolation period, increasing proportions of *Acinetobacter*, *Propionibacterium*,
519 *Rhizobium* and *Methylobacterium populi* were prevalent on the skin of the crew, while
520 signatures of *Pseudomonas*, *Corynebacterium* or unclassified *Intrasporangiaceae* decreased
521 (Supplementary Fig. S9).

522 **Dynamics of representative skin, GIT/UGT and environment-associated microbial taxa**

523 In a next step, we selected 15 microbial genera and families which were indicative of either
524 skin (*Acinetobacter*, *Staphylococcus [aureus]*, *Brevundimonas*, *Kocuria*, *Propionibacterium*,
525 *Streptococcus*, *Kytococcus*, Dermacoccaceae), gastrointestinal/urogenital tract (*Gardnerella*,
526 *Lactococcus*, *Methanobrevibacter*, *Faecalibacterium*, Enterobacteriaceae) or environment and
527 water (*Pseudomonas*, *Enhydrobacter*), to assess the dynamics of those microbial signatures.
528 Our feature selections were supported by higher rankings in differential abundance tests based
529 on gneiss, aldex2 and songbird, and feature loadings based on deicode. Grouping these
530 representative features into the categories skin, GIT/UGT (gastrointestinal/urogenital tract),
531 and environmental was based on empirical data from literature [10].

532 Representing the skin microbial taxa, *Acinetobacter*, despite being recognized as a typical skin
533 microbial taxon, shows higher relative abundances on built environment surfaces (especially
534 in the main room and bedroom). Crew member E showed over proportional prevalence at the
535 beginning and together with crew member A also at the end of the isolation period (Fig. 3B).

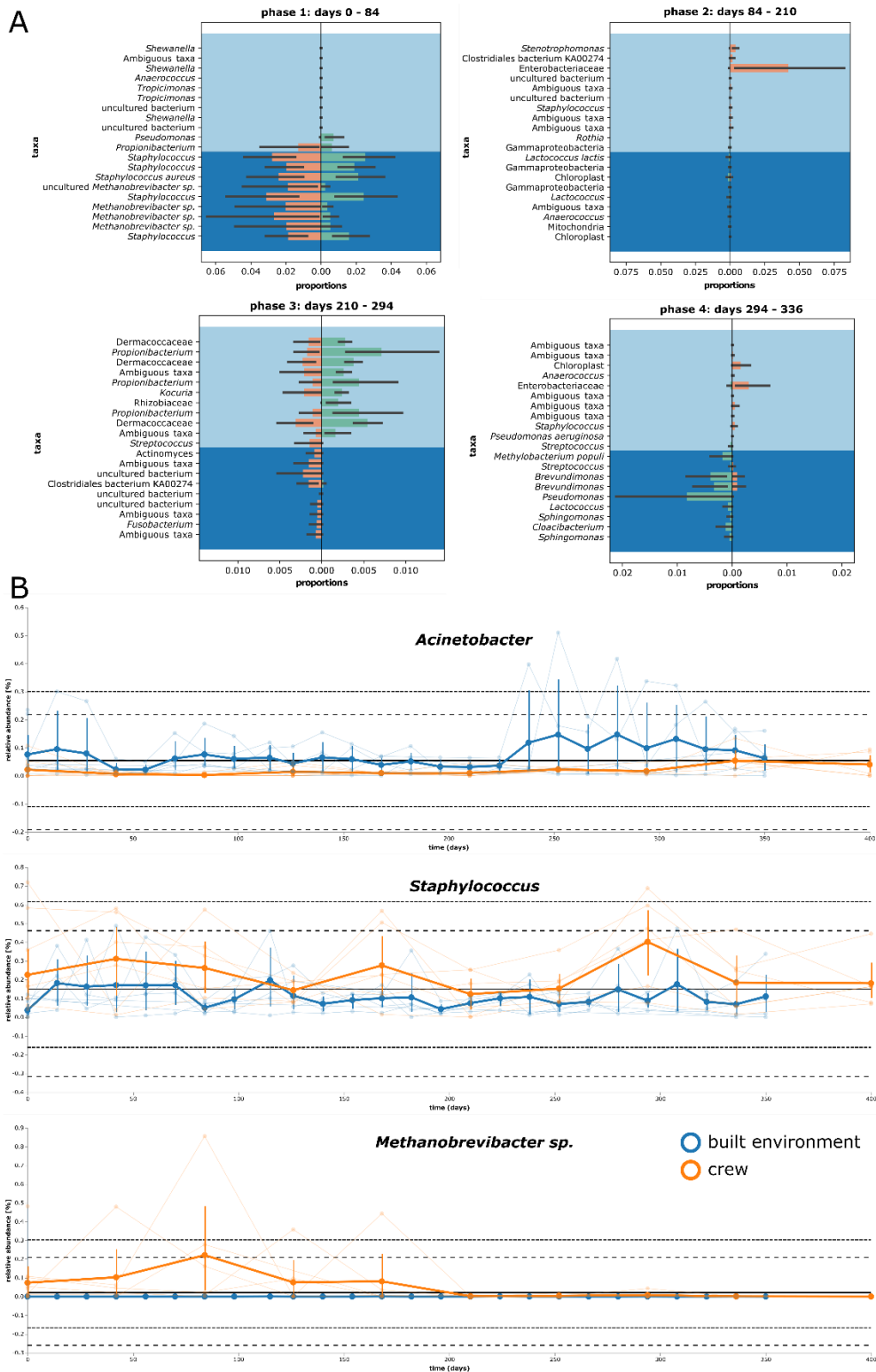
536 *Staphylococcus aureus* was mainly present on human skin (crew members D, E and F), but has
537 also been detected on surfaces inside the habitat. Interestingly, exchange with bedroom
538 surfaces seems obvious, since higher proportions of *S. aureus* on skin and bedroom surfaces
539 seem to be coupled (Fig. 3B and Supplementary Fig. S10). *Brevundimonas* was clearly
540 associated with the kitchen surfaces and could have been transferred to the toilet bowl (between
541 day 70 and day 84) and main room (between day 238 and day 252). Crew member F might
542 have picked up this taxon from the kitchen, for instance between day 238 and day 252 and
543 again between day 294 and day 336. Relative proportions of *Kocuria* were clearly correlated
544 with time by linear regression models and showed the highest value for importance (0.3). It
545 seems that this signature was introduced by crew members A and E into the habitat and then

546 transferred to almost all investigated built environment surfaces, as well as crew members B
547 and C. In contrast, *Propionibacterium* did not manifest itself on built environment surfaces
548 after being introduced by crew member D and was recovered only from other skin samples
549 over time. On the other hand, signatures of *Streptococcus* could not be linked to a defined
550 human source and established itself on bed and main room surfaces. *Kytococcus* was associated
551 with crew members A and D at the beginning. Later on, only single events of high proportions
552 were visible on the skin of crew member B or sampled bedroom surfaces, suggesting that this
553 taxon could not establish itself in the confined habitat. Dermacoccaceae could have been
554 continuously transferred between skin and built environment surfaces with a peak in the
555 bedroom and on crew member D at the end of the confinement period. After *Kocuria*,
556 Dermacoccaceae showed the highest importance (0.1) in linear regression models.

557 As a representative of the GIT/UGT, *Gardnerella* showed a consistent presence despite varying
558 proportions on the surface of the toilet bowl. Likewise, signatures of *Lactococcus* revealed a
559 single peak on the kitchen floor after day 50, but did not establish itself on the skin of any crew
560 member. In contrast to *Faecalibacterium*, *Methanobrevibacter* were not consistently recovered
561 from the toilet bowl, but were clearly associated with some of the crew members. As biplot
562 analyses identified Euryarchaeota (in particular *Methanobrevibacter* sp.) as the main reason
563 for compositional changes around day 84, this genus was analyzed further. In general,
564 signatures of *Methanobrevibacter* were highly associated with the human crew within the first
565 210 days (Fig. 3B and Supplementary Fig. S11). However, these signatures were not common
566 on built environment surfaces and were only observed on the toilet bowl and the kitchen floor
567 on day 115 and on day 224. This pattern was different from that of other archaeal lineages
568 (Euryarchaeota, Thaumarchaeota and Woesarchaeota), which showed scattered peaks on built
569 environment surfaces but not in skin samples. Enterobacteriaceae showed only single events
570 of prevalence on the toilet bowl and were mainly associated with skin samples of crew
571 members D, E and F between day 100 and day 250.

572 Despite representing an environment-associated taxon, *Enhydrobacter* was present on all crew
573 members to varying proportions and was regularly transferred to the toilet bowl. *Pseudomonas*
574 was obviously introduced by crew member B and D, then transferred to the kitchen floor and
575 further on to crew member E and F.

576



577

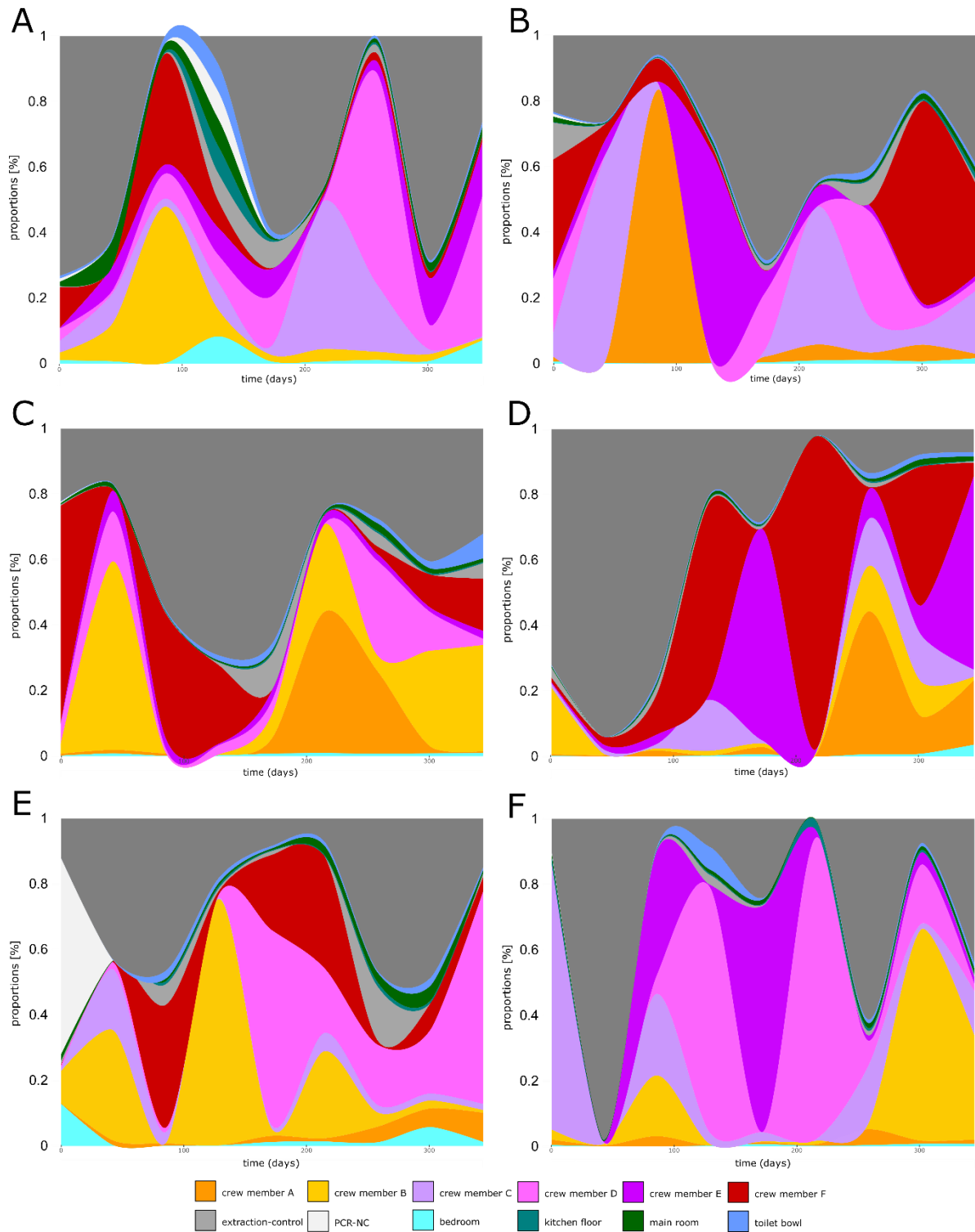
578 Fig. 3. Microbial dynamics in distinct phases and for representative features. A: Proportion plots of
 579 differential feature abundances using balances in gneiss on genus level grouped into four distinct phases.
 580 Background color of numerators light blue and for denominators dark blue. B: Volatility analysis based on linear
 581 regression models with time of *Acinetobacter*, *Staphylococcus* and *Methanobrevibacter* sp.

582

583 **Shared occupancy influences the microbiome composition and function of the crew skin**
584 **and abiotic surfaces**

585 Source tracking of microbial signatures with Sourcetracker2 identified human skin as the main
586 source of microbial dispersal. Noteworthy, the intensity of microbiome exchange was
587 heterogeneous among the possible pairs of crewmembers. In more detail, crew member F
588 showed the highest interactive profile (13.4%) of all crew members. This was also supported
589 by redundancy analysis (RDA) revealing pairwise microbial exchange for two pairs of
590 crewmembers as significant parameters on respective skin microbiome profiles ($p = 0.002$
591 RDA). Sampled locations of the built environment played only a minor role in overall microbial
592 dispersals. Maximal microbial contributions on the crew reached only proportions of 1.2% in
593 case of the main room. Interestingly, crew gender showed different microbial associations for
594 bedroom and the kitchen floor samples. Nevertheless, microbial interaction profiles were
595 highly person-specific as well as dynamic over time. Overall, trends were difficult to delineate
596 (Fig. 4).

597



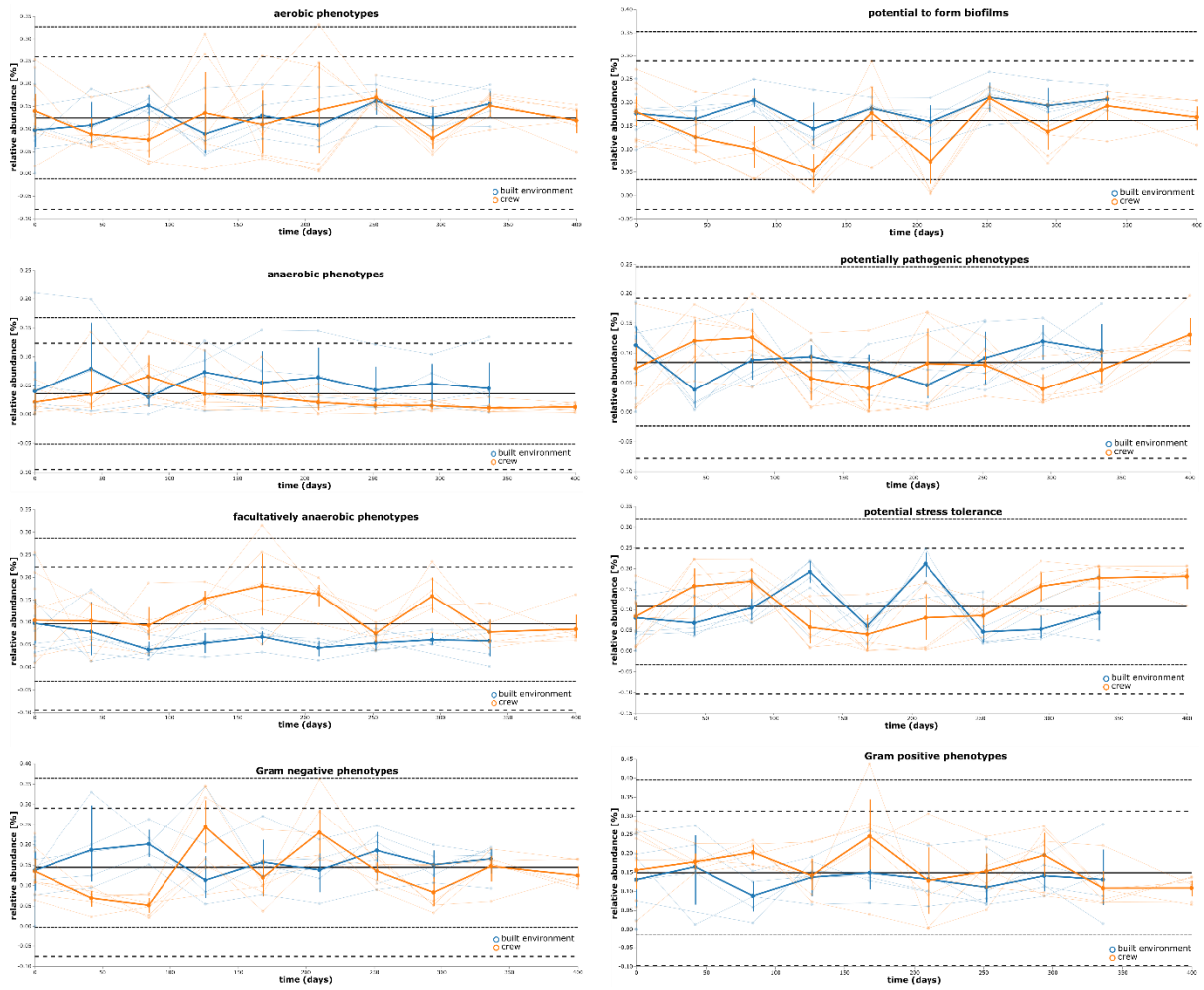
598

599 Fig. 4 Source tracking of microbial signatures according to SourceTracker2. Panels A to F show respective
 600 crew members A to F as a sink of microbial dispersal.

601

602 Further on, we were interested in whether microbial profiles and interactions between crew
603 members and surfaces inside the HI-SEAS habitat had an impact on potential phenotypes
604 predicted with Picrust 2 and BugBase. According to these predictions, most phenotypes
605 showed higher proportions (e.g., potential mobile elements, potential pathogens, potential
606 stress tolerance and especially facultative anaerobes) or recurring peaks (Gram-positive and
607 Gram-negative phenotypes and aerobes) on samples from the crew's skin. However, the
608 potential to form biofilms showed a constant maximum in samples retrieved from the kitchen
609 floor (global median 0.18, maximum 0.27, cumulative average decrease/increase -0.25/0.24)
610 and anaerobes were increasing on the toilet bowl (minimum 0.06, maximum 0.21) while
611 decreasing on human skin (0.02 to 0.01). Interestingly, potential pathogens showed an anti-
612 cyclic pattern of samples from the built environment versus samples from the crew (Fig. 5).

613



614

615 Fig. 5. Linear regression with time of predicted phenotypes from BugBase shown as volatility plots (sorted
 616 according to regression with time).

617

618 **Fluctuation of microbial quantity correlates with the presence of certain antimicrobial**
619 **resistance genes and microbial phenotypes**

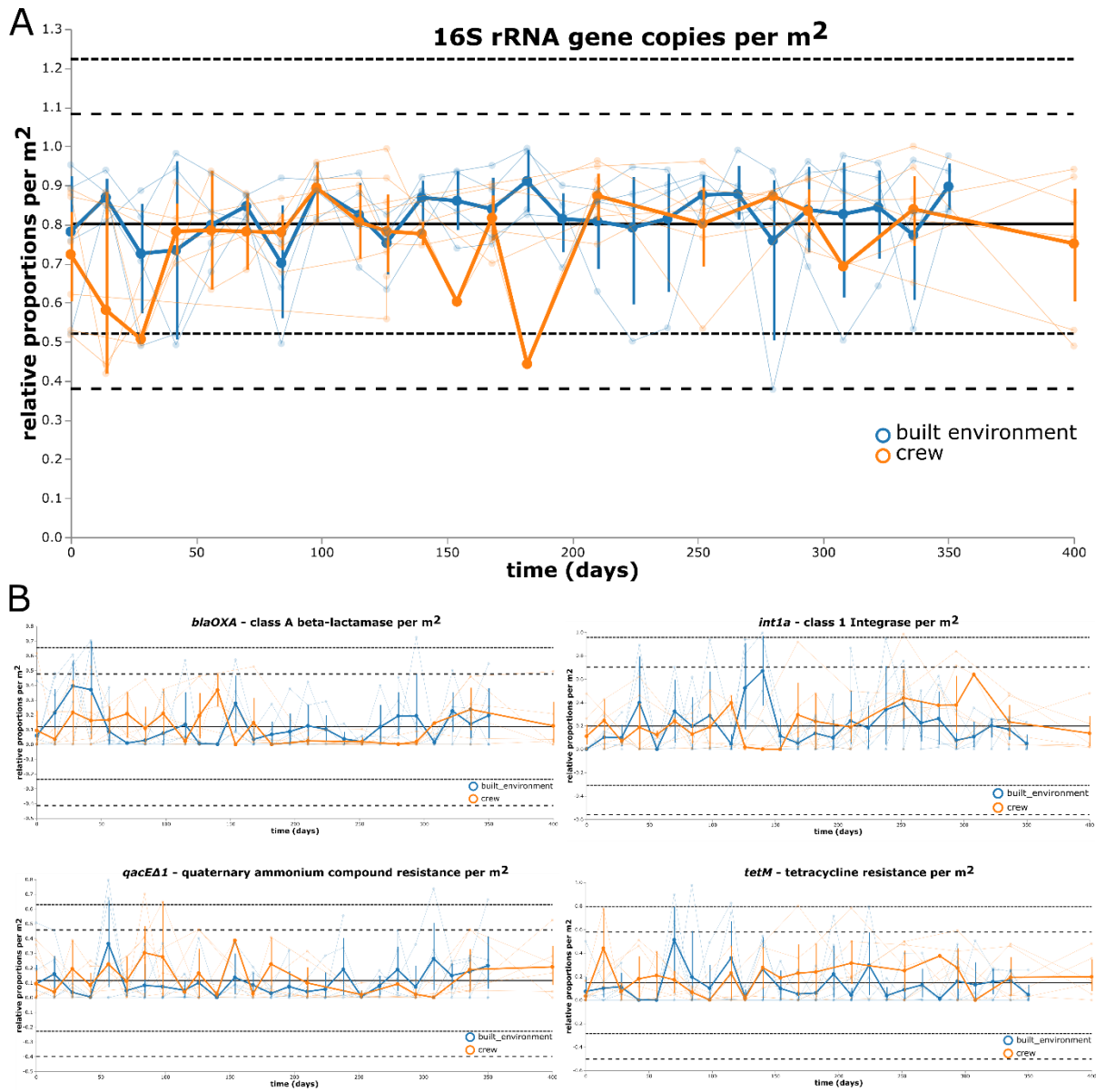
620 Quantitative PCR was used to assess bacterial and archaeal abundance, and its dynamics inside
621 the HI-SEAS habitat and the skin of its isolated crew members. As observed for microbial
622 profiles, bacterial abundance changed to a larger extent for samples from the crew's skin than
623 from built environment surfaces. In general, two main phases of differing bacterial load could
624 be determined. In the beginning (days 0 - 42) and between days 126 and 210, bacterial
625 abundance on human skin was much lower than on selected locations of the built environment
626 (respective mean difference for the two phases: 12.5 and 22.5%). The largest dynamics were
627 observed around day 28 and day 182 (change in relative proportions by 43%; Fig. 6A). On the
628 other hand, archaeal abundance peaked around day 84 (82%) but varied to much lesser extents,
629 especially in the mid-term of the isolation period (Supplementary Fig. S12).

630 In addition, four markers for antimicrobial resistance (*blaOXA* - class A beta-lactamase, *intIa*
631 - class 1 integrase, *qacEΔI* - biocide resistance gene, quaternary ammonium compound and
632 *tetM* - tetracycline resistance) were selected to analyze dynamics of microbial resistances in a
633 quantitative way. *TetM* was most predictive for the factor time (importance = 0.2) and was
634 constantly more abundant in skin samples between day 140 and day 294. Interestingly, beta-
635 lactamases showed the opposite pattern, with lowest proportions between day 140 to day 294.
636 *IntIa* gene abundance was highly dynamic over the whole time frame (highest global variance
637 of 0.06) and showed peaks on built environment locations (toilet bowl and kitchen floor) on
638 day 140, but also on human skin (especially crew member C and D) on day 308. Highest and
639 lowest abundances of *qacEΔI* regularly alternated between samples of the built environment
640 and from human skin. Nevertheless, all four targeted resistance genes showed high dynamics
641 and potential transfer between skin and the built environment (Fig. 6B).

642 Finally, predicted phenotypes were correlated both with each other and with obtained
643 quantitative information (16S rRNA gene copies and selected resistance genes). While all
644 quantitative data could be significantly positively correlated with each other (especially class
645 A beta-lactamases with biocide resistance of quaternary ammonium compounds - $P = 5.0 \cdot 10^{-15}$, $\rho = 0.66$), and biocide resistance of quaternary ammonium compounds with tetracycline
646 resistance - $P = 3.2 \cdot 10^{-8}$, $\rho = 0.5$), comparisons of the qualitative information showed both
647 positive and negative correlations. Significant positive correlations were evident between
648 aerobes and potential biofilm formers ($P = 4.9 \cdot 10^{-12}$, $\rho = 0.60$), as well as potential
649

650 pathogens and stress tolerance ($P = 2.1 \times 10^{-13}$, $\rho = 0.63$). On the contrary, significant
651 negative correlations were observed between aerobes and facultative anaerobes ($P = 2.2 \times 10^{-16}$,
652 $\rho = -0.67$), as well as between potential biofilm formers and Gram-positives ($P =$
653 1.1×10^{-8} , $\rho = -0.51$). However, significant correlations between quantitative and qualitative
654 measures were scarce. Only the overall bacterial load (16S rRNA gene copy numbers) showed
655 significant positive correlations with anaerobes ($P = 5.6 \times 10^{-4}$, $\rho = 0.32$) and significant
656 negative correlations with aerobes ($P = 5.3 \times 10^{-3}$, $\rho = -0.26$).

657



658

659 Fig. 6. Overall bacterial load and abundance of selected antimicrobial resistances. A: Volatility analysis of
 660 bacterial 16S rRNA gene copies per m² according to qPCR. B: Linear regression volatility analysis of selected
 661 resistance gene copies per m² according to qPCR.

662

663

664 Discussion

665

666 Human well-being is inseparably linked with its microbiome. Thus, the dynamics of the
667 microbiome in and around a human being is subject of research for the preparation of human
668 long-term spaceflight and settlement in remote locations such as a future Martian outpost [7].
669 For such studies, Earth-based models are indispensable including a monitoring of the
670 longitudinal microbial dynamics of an isolated crew with its confined environment beside
671 social analysis of team cohesion and performance. Numerous suitable model environments
672 were investigated in the past (besides the one studied herein), but greatly differed in terms of
673 setup and study design. For instance, the Concordia research station in Antarctica comprised
674 separate buildings, accommodated 16-32 occupants during the sampling period and was
675 microbially monitored for 365 days [43]. The US inflated lunar/Mars analog habitat (ILMAH)
676 provided 300 m³ space for three occupants and was investigated for 30 days [44]. Another
677 example is the Mars500 habitat located in Moscow, Russia, which included four modules with
678 a total volume of 550 m³ and housed six participants for 520 days [41].

679 All isolated and confined built environment (ICE) models represented a unique testbed for
680 assessing the microbial interaction of an isolated crew inside a confined built environment. In
681 contrast to other studies in the MoBE (microbiology of built environments) field, its reduced
682 set of potential environmental variables that could drive the microbiome in a longitudinal
683 context allows distinct assumptions about where microbial signatures originated, as well as
684 when, where and why they were transferred through time and space [83].

685 Unexpectedly, our study revealed a highly dynamic skin microbiome of the HI-SEAS crew
686 despite its isolated and confined setup. In contrast to the study by Sharma and co-workers [81]
687 in which longitudinal homogenization of microbial composition was visible *ab initio*, we
688 observed a retarded longitudinal homogenization between skin and built environment samples
689 only after 210 days. Nevertheless, traces of the skin microbiome were clearly visible on the
690 studied surfaces and as described before occupancy was identified as the major microbial
691 source [9,84–86]. Compared to microbial interaction profiles from human skin, building
692 surfaces seem to play a more passive and subordinated role for spreading and dispersal in this
693 habitat and confirmed again that humans dominate microbial communities on indoor surfaces
694 [87,88]. Accordingly, the kitchen floor surface stood out with its low microbial diversity. This

695 observation could be associated with the low interaction frequency of this specific location
696 (floor surface) in contrast to the regularly touched desk or toilet surfaces in the habitat.

697 In contrast to other isolation experiments like the Mars500 study [41] in which a significant
698 decrease in microbial diversity was observed, the microbial diversity on the HI-SEAS surfaces
699 remained rather constant and even increased in samples from crew skin. Confirmed by our
700 meta-analysis based on four selected longitudinal studies from built environment settings,
701 increasing microbial diversity on human skin and built environment samples was not reported
702 in offices or homes [80,82]. However, this observation could be the result of a human
703 occupancy in confined and in more isolated built environments as this pattern was also
704 observed in samples from crew members at the ISS (International Space Station) for samples
705 of the forearm and gut [89] or in fecal samples during the cohabitation of US Air Force cadets
706 [81]. Crew members C, D, E, and F started with a relatively low range of microbial diversity
707 on their skin compared to representative studies of the skin microbiome[90,91]. This rather low
708 microbial diversity might result from extensive personal hygiene cleaning procedures before
709 entering the HI-SEAS habitat with a limited allowance of daily hygiene procedures.

710 The sources of microorganisms are not completely clear; the steady increase on the crew's skin
711 could result from interactions with the higher microbial diversity present in their habitat (refer
712 to Fig. 2A and 2B), regular resupply events, complications and elaborate cleaning of the
713 composting toilet (for details see below) or dispersal of microbial food supplements used to
714 ferment food. In addition to these potential microbial sources, the altered hygiene regime
715 during isolation has probably contributed to an increase or stabilization of skin microbiome
716 composition. The most stable skin microbiome was observed for a crew member, who applied
717 extremely short showers (average duration of 40 seconds; Supplementary Table S4), compared
718 to the other crew members (overall average showering time of 102 seconds), which revealed a
719 more fluctuating microbial profile. Another impact of hygiene regimens on the skin
720 microbiome was indicated by the higher abundance of quaternary ammonium compound
721 resistance genes on the skin of individual crew members. This observation reflected the
722 application of disinfecting cleaning wipes (which contained such compounds) on the crew's
723 skin in-between the showering events.

724 The most striking observation was the delayed longitudinal homogenization and very dynamic
725 developments of the skin microbiome in the first half of the isolation period (days 0 – 210).
726 These unstable profiles correlated with complications of the composting toilet, which required

727 a manual cleaning and emptying rotationally by all the crew members. Dispersal of
728 gut/urogenital-associated microorganisms from the composting toilet might have even been
729 supported by the use of a fan to reduce the odor. An obvious indicator species of these
730 complications was *Methanobrevibacter*. As verified by biplots, specific filtering of the dataset
731 and significant correlations of quantitative data (bacterial and archaeal abundance) with an
732 anaerobic predicted phenotype, this archaeon of the human gut explained most of the dynamics
733 in this timeframe and delayed the expected longitudinal homogenization process of its
734 microbiome. *Methanobrevibacter* represents the most common archaeal genus of the human
735 gut and has an important role at the end of the intestinal food chain where it facilitates the
736 fermentation process of bacteria by removing hydrogen from the system (an overview is given
737 in [92]. Obviously, the increased prediction of anaerobic phenotypes correlated very well with
738 the increased signatures of *Methanobrevibacter* in the same timeframe. Later on, the signatures
739 of *Methanobrevibacter* increased relatively on samples of the toilet bowl while decreasing on
740 human skin as soon as the toilet issue was fixed. Most of the other predicted phenotypes showed
741 higher relative proportions and dynamics on skin samples, which might be due to the reported
742 temporal and personalized variability on human skin samples [90,93]. In addition, the anti-
743 cyclic pattern of potential pathogens might picture regular transfer events between skin and
744 desk surfaces in the habitat, which were described before [81].

745 Besides the remarkable traces of gut-associated archaea, other selected bacterial indicator
746 species were helpful to interpret microbial dynamics in the HI-SEAS habitat. Hence, most skin-
747 associated bacteria like *Staphylococcus aureus*, *Brevundimonas*, *Kocuria*, *Propionibacterium*,
748 *Streptococcus*, *Kytococcus* and Dermacoccaceae could be easily traced in the habitat, were most
749 frequently exchanged with the desk surface in the bedroom and were transferred more likely
750 between crew members who also had close physical interaction with each other. Their presence
751 on different built environment locations were often transient and higher proportions were
752 usually detected in samples from the crew. This observation was also confirmed by source
753 tracking analysis, which showed higher microbial transfer between crew members A and D, B
754 and C, or E and F, or low microbial transfer between crew members A and F, or C and E. This
755 microbial transfer pattern corresponds to the reported interaction preference of male with
756 female crew members during the isolation period. These results underline the important impact
757 of the personal microbial cloud [94], the importance of direct physical interaction [80,95,96]
758 as well as cohabitation of crew members [97] and the low microbial input from selected built
759 environment locations [88] to the overall microbiome of the HI-SEAS habitat.

760 *Propionibacterium* could act as an example for the low input of the built environment
761 microbiome, since this bacterium was only recovered from skin samples and was never
762 observed on surfaces of the HI-SEAS habitat. This might be due to its strict anaerobic lifestyle,
763 that seems to prefer the oxygen depleted pores of human skin and much less those relatively
764 smooth oxygen rich building surfaces and materials.

765 However, an opposite profile was observed for signatures of *Acinetobacter*. Although
766 described as a skin-associated microbe [98], *Acinetobacter* established itself much better in
767 various locations of the main room and bedroom. As this bacterium is also frequently detected
768 on surfaces of public and private buildings, as well as hospitals or cleanrooms [99–102] it is
769 tempting to speculate whether *Acinetobacter* could be perceived as an indicator species for
770 confined built environments and to a lesser extent only as a skin-associated bacterium.

771 Peaks of signatures from *Lactococcus* on the kitchen floor might be due to its usage in
772 fermenting yoghurt, cream cheese (*Lactococcus lactis* subsp. *lactis* and *cremoris*), tempeh or
773 kombucha. The idea of using microbial cultures as part of the food supply, or entire artificial
774 ecosystems for life support [28,103], is of particular importance in ICE and might be key to
775 colonize another celestial body in the solar system. Nevertheless, the exact composition of
776 commercially available products must be well-characterized to mitigate potential risks for the
777 crew.

778 Although a number of metadata about health and medication of the crew were obtained, the
779 information was not precise enough for correlations with the microbiome. Crew members
780 provided medication data, but only two reported treatments could be associated with increases
781 in tetracycline resistance and bacterial abundances, potential pathogens or stress tolerance.
782 Hence, in contrast to the study by Abeles and co-workers [104] who could follow specific
783 treatment courses in the microbiome, our dataset was not comprehensive enough to make such
784 assumptions. On the contrary, recordings of the microclimate produced numerous values, but
785 was rather constant and did not represent a major driving factor of the microbiome (only up to
786 9%) as investigated by bioenv analysis.

787 The presented study has limitations and serves only partially as a basis for meaningful
788 recommendations for future attempts to sustain a safe microbial environment in a human
789 outpost on the Moon or Mars. First of all, no baseline (i.e. before the start of the isolation
790 experiment) of the indoor and skin microbiome was defined. In addition, information on all

791 microbial sources were limited and only one body site was selected for monitoring potential
792 microbial transfer with the environment. Additional human samples would have been
793 supportive to draw conclusions about an individual's health status (e.g. fecal samples) or draw
794 detailed conclusions of frequently touched surfaces inside the habitat (e.g. hand samples).

795 Nevertheless, the study benefits from its defined confined setup with limited amount of
796 confounding environmental variables, a defined set of occupants, the deduced prediction and
797 tracking potential of microbial transfer in a remarkable level of detail, the correlation of
798 qualitative and quantitative microbial and resistance data and our pre-informed knowledge of
799 microbial hotspots on desks, in bedrooms, or the toilet bowl on ICE locations from the Mars500
800 project [41].

801

802 **Conclusions**

803 From a microbiological point of view, the risk of infection or transfer of antimicrobial resistant
804 pathogens to crew members was found to be extraordinarily low and is thus in agreement with
805 recent information from the ISS [24]. However, although the risk was deemed to be low, the
806 need for monitoring microbial dynamics inside isolated and confined habitats became obvious,
807 in order to understand the impact of special events like the contamination caused by the
808 composting toilet. Moreover, baselines of the microbiome inside the habitat, its crew and post
809 sampling events would greatly improve evaluations of the impact of confinement on the crew
810 and habitat surfaces. Most comparable studies, either ground-based like Mars500 [41,105] or
811 in space aboard the ISS [24,89,106], showed a similar picture of longitudinal homogenization,
812 composition and diversity of microbiomes.

813 However, in many cases these studies suffered from a lack of appropriate controls, or baselines,
814 which are a central point of management of metadata or interpretations. For future experiments,
815 it is key to determine a standard operating procedure regarding sampling intervals, methods
816 suitable for microbial monitoring, distinct knowledge on pre- or probiotics used for food
817 production, stabilization of the gut microbiome or even personalized collections for autologous
818 fecal microbial transplants in case of worrisome developments leading to a microbial dysbiosis.
819 Hence, future ICE missions in preparation for crewed mission to the Moon or Mars in the
820 upcoming decades should emphasize on actual tests on a microbial warning system that could
821 be based on automatic sampling technologies as developed by BiomeSense
822 (<https://www.biomesenseinc.com/>) and predictive models comparing expected and true
823 microbial compositions in the habitat and its crew. Furthermore, manipulations of the
824 microbiome would be essential to stress the microbiome by different levels of desired (reduce
825 potential pathogens and technophilic microorganisms) and unintentional perturbations through
826 defined cleaners and antibiotics, and following restorations of a beneficial community on the
827 surfaces of the habitat, as well as different body sites including the crew's gut microbiome.
828 One key question for future related studies is how diverse a microbiome needs to be and which
829 actual composition it needs to have on surfaces, and on and in the human body, to be self-
830 sustaining over longer timeframes, or how it can be stabilized and restored after critical
831 perturbations. The answers to these questions are a crucial prerequisite for the planning of
832 future human long-term missions in space or on other celestial bodies in our solar system.

833 **List of abbreviations**

- 834 ANCOM: Analysis of composition of microbiomes
- 835 ASVs: Amplicon sequence variants
- 836 BHP: Behavioral Health and Performance
- 837 CSA: Canadian Space Agency
- 838 FDR: False discovery rate
- 839 HI-SEAS: Hawaii Space Exploration Analog and Simulation mission
- 840 ICE: Isolated and confined built environments
- 841 ILMAH: Inflatable lunar/Mars analogous habitat
- 842 ISS: International Space Station
- 843 JAXA: Japan Aerospace Exploration Agency
- 844 LEfSe: Linear discriminant analysis Effect Size
- 845 MoBE: Microbiome of the built environment
- 846 NASA: National Aeronautics and Space Administration
- 847 PCR: Polymerase chain reaction
- 848 qPCR: Quantitative polymerase chain reaction
- 849 PERMANOVA: Permutational multivariate analysis of variance
- 850 QIIME: Quantitative Insights Into Microbial Ecology
- 851 RDA: Redundancy analysis
- 852 SD: Standard deviation
- 853

854 **Declarations**

855

856 Ethics approval and consent to participate

857 The study proposal was reviewed and approved by an institutional review board (JSC IRB -
858 Study Protocol Number 1648: Key contributors to the maintenance and regulation of team
859 function and performance on long duration missions).

860

861 Consent for publication

862 All authors gave their consent for publications.

863

864 Availability of data and materials

865 All the raw and processed data used for analyses in this study have been deposited in QIITA
866 under the study ID 12858 (<https://qiita.ucsd.edu/>; Gonzalez et al., 2018) and EBI-ENA under
867 the accession number ERP118380.

868 Competing interests

869 The authors declare that they have no competing interests.

870

871 Funding

872 This research was supported in part by NASA Grant NNX13AM78G and by the Europlanet
873 2020 RI (Project No 11219). Europlanet 2020 RI has received funding from the European
874 Union's Horizon 2020 research and innovation program under grant agreement No 654208.

875 CV acknowledges support from the Alexander von Humboldt Foundation.

876

877 Authors' contributions

878 AM, CM-E, CV wrote the manuscript. AM, CM-E analyzed the data. CV, PS, DBi, CM-E
879 did the study design. CV, KK, LW, DBr, TG, CK, MB did the work in the wet-lab. All

880 authors improved the manuscript by their specific input and also approved the final version of
881 the manuscript.

882

883 Acknowledgements

884 We thank Anna Schwarz for lab support, the HI-SEAS staff and mission support for facilitating
885 the project, the HI-SEAS IV crewmembers for taking part in the study and providing metadata,
886 and Michaela Musilova for her help in retrieving further metadata. Christiane Heinicke
887 recorded and kindly provided data on shower use. We also wish to acknowledge the support of
888 Henk Rogers and Paul Ponthieux (Blue Planet Foundation), and Bill Wiecking (Hawaii
889 Preparatory Academy) to the HI-SEAS IV mission.

890

891

892 **References**

- 893 1. Trump D. Space Policy Directive 1: Reinvigorating America's Space
894 Exploration Program. 2017 p. Federal Register 82(239): 59501–2.
- 895 2. NASA. NASA's FY2020 Budget Amendment Summary. 2019.
- 896 3. Woerner J, Foing B. The 'Moon Village' Concept and Initiative." LPI
897 Contributions 1960 2016.
- 898 4. ESA. Resolution on ESA programmes: addressing the challenges ahead.
899 ESA/C-M/CCLXXXVI/Res.3. 2019.
- 900 5. Crawford IA. Science enabled by a Moon Village. 2017; Available from:
901 <http://arxiv.org/abs/1706.06698>
- 902 6. Heinicke C, Jaret S, Ormö J, Fateri M, Kopacz N, Baqué M, et al. How a
903 laboratory on the Moon should be equipped. 69th Int Astronaut Congr (IAC),
904 IAC-18-F123. 2018;1–5.
- 905 7. Musk E. Making Humans a Multi-Planetary Species. *New Sp.* 2017;5:46–61.
- 906 8. Sender R, Fuchs S, Milo R. Are We Really Vastly Outnumbered? Revisiting
907 the Ratio of Bacterial to Host Cells in Humans. *Cell* [Internet]. Elsevier Inc.;
908 2016;164:337–40. Available from: <http://dx.doi.org/10.1016/j.cell.2016.01.013>
- 909 9. Qian J, Hospodsky D, Yamamoto N, Nazaroff WW, Peccia J. Size-resolved
910 emission rates of airborne bacteria and fungi in an occupied classroom. *Indoor*
911 *Air* [Internet]. 2012 [cited 2014 Jan 24];22:339–51. Available from:
912 <http://www.pubmedcentral.nih.gov/articlerender.fcgi?artid=3437488&tool=pmc>
913 [entrez&rendertype=abstract](http://www.pubmedcentral.nih.gov/articlerender.fcgi?artid=3437488&tool=pmc&rendertype=abstract)
- 914 10. Lloyd-Price J, Abu-Ali G, Huttenhower C. The healthy human microbiome.
915 *Genome Med* [Internet]. *Genome Medicine*; 2016;8:1–11. Available from:

- 916 <http://dx.doi.org/10.1186/s13073-016-0307-y>
- 917 11. Weinstein R, Mermel LA. Infection prevention and control during
918 prolonged human space travel. *Clin Infect Dis*. 2013;56:123–30.
- 919 12. Horneck G, Klaus DM, Mancinelli RL. Space Microbiology. *Microbiol Mol*
920 *Biol Rev*. 2010;74:121–56.
- 921 13. Ott M, Pierson D, Shirakawa M, Tanigaki F, Hida M, Yamazaki T, et al.
922 Space Habitation and Microbiology: Status and Roadmap of Space Agencies.
923 *Microbes Environ* [Internet]. 2014;00:1–4. Available from:
924 <http://jlc.jst.go.jp/DN/JST.JSTAGE/jsme2/ME2903rh?lang=en&from=CrossRef>
925 [&type=abstract](http://jlc.jst.go.jp/DN/JST.JSTAGE/jsme2/ME2903rh?lang=en&from=CrossRef)
- 926 14. Taylor PW. Impact of space flight on bacterial virulence and antibiotic
927 susceptibility. *Infect Drug Resist*. 2015;8:249–62.
- 928 15. Aponte VM, Finch DS, Klaus DM. Considerations for non-invasive in-flight
929 monitoring of astronaut immune status with potential use of MEMS and NEMS
930 devices. *Life Sci*. 2006;79:1317–33.
- 931 16. Fajardo-Cavazos P, Nicholson WL. Cultivation of *Staphylococcus*
932 *epidermidis* in the human spaceflight environment leads to alterations in the
933 frequency and spectrum of spontaneous rifampicin-resistance mutations in the
934 *rpoB* gene. *Front Microbiol*. 2016;7:1–10.
- 935 17. Mehta SK, Laudenslager ML, Stowe RP, Crucian BE, Sams CF, Pierson
936 DL. Multiple latent viruses reactivate in astronauts during Space Shuttle
937 missions. *Brain Behav Immun* [Internet]. Elsevier Inc.; 2014;41:210–7.
938 Available from: <http://dx.doi.org/10.1016/j.bbi.2014.05.014>
- 939 18. Mora M, Mahnert A, Koskinen K, Pausan MR, Oberauner-Wappis L,
940 Krause R, et al. Microorganisms in Confined Habitats: Microbial Monitoring

941 and Control of Intensive Care Units, Operating Rooms, Cleanrooms and the
942 International Space Station. *Front Microbiol.* 2016;7:1–20.

943 19. Novikova N, De Boever P, Poddubko S, Deshevaya E, Polikarpov N,
944 Rakova N, et al. Survey of environmental biocontamination on board the
945 International Space Station. *Res Microbiol.* 2006;157:5–12.

946 20. Heppener M. Spaceward ho! The future of humans in space. *EMBO Rep.*
947 2008;9.

948 21. Gu JD. Microbial colonization of polymeric materials for space applications
949 and mechanisms of biodeterioration: A review. *Int Biodeterior Biodegrad.*
950 2007;59:170–9.

951 22. Alekhova TA, Aleksandrova AA, Novozhilova TY, Lysak L V., Zagustina
952 NA, Bezborodov AM. Monitoring of microbial degraders in manned space
953 stations. *Appl Biochem Microbiol.* 2005;41:382–9.

954 23. Novikova ND. Review of the knowledge of microbial contamination of the
955 Russian manned spacecraft. *Microb Ecol [Internet]*. 2004 [cited 2012 Sep
956 24];47:127–32. Available from: [http://link.springer.com/article/10.1007/s00248-](http://link.springer.com/article/10.1007/s00248-003-1055-2)
957 003-1055-2

958 24. Mora M, Wink L, Kögler I, Mahnert A, Rettberg P, Schwendner P, et al.
959 Space Station conditions are selective but do not alter microbial characteristics
960 relevant to human health. *Nat Commun [Internet]*. Springer US; 2019;10.
961 Available from: <http://dx.doi.org/10.1038/s41467-019-11682-z>

962 25. Klintworth R, Reher HJ, Viktorov AN, Bohle D. Biological induced
963 corrosion of materials II: new test methods and experiences from MIR station.
964 *Acta Astronaut [Internet]*. 1999 [cited 2012 Sep 24];44:569–78. Available from:
965 <http://www.sciencedirect.com/science/article/pii/S0094576599000697>

- 966 26. Marche C, Guarnieri V, Gaia E, Battocchio L, Pitzurra M. New methods for
967 microbial contamination monitoring: an experiment on board the MIR orbital
968 station. *Acta Astronaut* [Internet]. 1997 [cited 2012 Sep 24];40:195–201.
969 Available from:
970 <http://www.sciencedirect.com/science/article/pii/S0094576597001021>
- 971 27. Sun Y, Xie B, Wang M, Dong C, Du X, Fu Y, et al. Microbial community
972 structure and succession of airborne microbes in closed artificial ecosystem.
973 *Ecol Eng* [Internet]. Elsevier B.V.; 2016;88:165–76. Available from:
974 <http://dx.doi.org/10.1016/j.ecoleng.2015.12.013>
- 975 28. Lasseur C, Brunet J, Weever H De, Dixon M, Dussap G, Godia F, et al.
976 Melissa: The European project of closed life support system. *Gravitational Sp*
977 *Biol* [Internet]. 2010;23:3–12. Available from:
978 <http://adsabs.harvard.edu/abs/2006cosp...36.3579L>
- 979 29. Tikhomirov AA, Ushakova SA, Kovaleva NP, Lamaze B, Lobo M, Lasseur
980 C. Biological life support systems for a Mars mission planetary base: Problems
981 and prospects. *Adv Sp Res*. 2007;40:1741–5.
- 982 30. Verseux C, Baqué M, Lehto K, De Vera JPP, Rothschild LJ, Billi D.
983 Sustainable life support on Mars - The potential roles of cyanobacteria. *Int J*
984 *Astrobiol*. 2016;15:65–92.
- 985 31. COSPAR. COSPAR Planetary Protection Policy [Internet]. 2011. Available
986 from: <https://cosparhq.cnes.fr/sites/default/files/pppolicy.pdf>.
- 987 32. Horneck G. The microbial case for Mars and its implication for human
988 expeditions to Mars. *Acta Astronaut*. 2008;63:1015–24.
- 989 33. Moissl-Eichinger C, Rettberg P, Pukall R. The First Collection of
990 Spacecraft-Associated Microorganisms: A Public Source for Extremotolerant

991 Microorganisms from Spacecraft Assembly Clean Rooms. *Astrobiology*.
992 2012;12:1024–34.

993 34. Moissl-Eichinger C, Auerbach AK, Probst AJ, Mahnert A, Tom L, Piceno
994 Y, et al. Quo vadis? Microbial profiling revealed strong effects of cleanroom
995 maintenance and routes of contamination in indoor environments. *Sci Rep*.
996 2015;5:9156.

997 35. Mora M, Perras AK, Alekhova TA, Wink L, Krause R, Aleksandrova A, et
998 al. Resilient microorganisms in dust samples of the International Space Station
999 – Survival of the adaptation specialists. *Microbiome* [Internet]. *Microbiome*;
1000 2016;4:1–21. Available from: <http://dx.doi.org/10.1186/s40168-016-0217-7>

1001 36. Castro VA, Thrasher AN, Healy M, Ott CM, Pierson DL. Microbial
1002 characterization during the early habitation of the International Space Station.
1003 *Microb Ecol* [Internet]. 2004 [cited 2012 Sep 24];47:119–26. Available from:
1004 <http://www.ncbi.nlm.nih.gov/pubmed/14749908>

1005 37. Checinska A, Probst AJ, Vaishampayan P, White JR, Kumar D, Stepanov
1006 VG, et al. Microbiomes of the dust particles collected from the International
1007 Space Station and Spacecraft Assembly Facilities. *Microbiome* [Internet].
1008 *Microbiome*; 2015;3:50. Available from: [http://dx.doi.org/10.1186/s40168-015-](http://dx.doi.org/10.1186/s40168-015-0116-3)
1009 0116-3

1010 38. Coil DA, Neches RY, Lang JM, Brown WE, Severance M, Cavalier D, et al.
1011 Growth of 48 built environment bacterial isolates on board the International
1012 Space Station (ISS). *PeerJ*. 2016;2016:1–11.

1013 39. Urbaniak C, Sielaff AC, Frey KG, Allen JE, Singh N, Jaing C, et al.
1014 Detection of antimicrobial resistance genes associated with the International
1015 Space Station environmental surfaces. *Sci Rep* [Internet]. Springer US;
1016 2018;8:1–13. Available from: <http://dx.doi.org/10.1038/s41598-017-18506-4>

- 1017 40. Venkateswaran K, Vaishampayan P, Cisneros J, Pierson DL, Rogers SO,
1018 Perry J. International Space Station environmental microbiome - microbial
1019 inventories of ISS filter debris. *Appl Microbiol Biotechnol*. 2014;98:6453–66.
- 1020 41. Schwendner P, Mahnert A, Koskinen K, Moissl-Eichinger C, Barczyk S,
1021 Wirth R, et al. Preparing for the crewed Mars journey: microbiota dynamics in
1022 the confined Mars500 habitat during simulated Mars flight and landing.
1023 *Microbiome*. 2017;5.
- 1024 42. Schwendner P. MICROBIAL ECOLOGY OF THE MARS 500 HABITAT.
1025 Regensburg University; 2014.
- 1026 43. Houdt R Van, Boever P De, Coninx I. Evaluation of the airborne bacterial
1027 population in the periodically confined Antarctic base Concordia. *Microb Ecol*
1028 [Internet]. 2008 [cited 2012 Sep 24];57:640–8. Available from:
1029 <http://www.springerlink.com/index/17553042j6u0852q.pdf>
- 1030 44. Mayer T, Blachowicz A, Probst AJ, Vaishampayan P, Checinska A,
1031 Swarmer T, et al. Microbial succession in an inflated lunar/Mars analog habitat
1032 during a 30-day human occupation. *Microbiome* [Internet]. *Microbiome*;
1033 2016;4:1–17. Available from: <http://dx.doi.org/10.1186/s40168-016-0167-0>
- 1034 45. Caldwell BJ, Roma PG, Binsted K. Team Cohesion, Performance, and
1035 Biopsychosocial Adaptation Research at the Hawaii Space Exploration Analog
1036 and Simulation (HI-SEAS). 31st Annu Conf Soc Ind Organ Psychol. 2016;
- 1037 46. Caporaso JG, Lauber CL, Walters WA, Berg-Lyons D, Huntley J, Fierer N,
1038 et al. Ultra-high-throughput microbial community analysis on the Illumina
1039 HiSeq and MiSeq platforms. *ISME J* [Internet]. Nature Publishing Group;
1040 2012;6:1621–4. Available from: <http://dx.doi.org/10.1038/ismej.2012.8>
- 1041 47. Bolyen E, Rideout JR, Dillon MR, Bokulich NA, Chase J, Cope EK, et al.

1042 Reproducible, interactive, scalable and extensible microbiome data science
1043 using QIIME 2. *Nat Biotechnol.* 2019;37:852–7.

1044 48. Callahan BJ, Mcmurdie PJ, Rosen MJ, Han AW, Johnson AJ, Holmes SP.
1045 DADA2: High resolution sample inference from amplicon data. *Nat Methods.*
1046 Nature Publishing Group; 2016;13:581–3.

1047 49. Davis NM, Proctor DiM, Holmes SP, Relman DA, Callahan BJ. Simple
1048 statistical identification and removal of contaminant sequences in marker-gene
1049 and metagenomics data. *Microbiome.* *Microbiome*; 2018;6:1–14.

1050 50. Bokulich NA, Kaehler BD, Rideout JR, Dillon M, Bolyen E, Knight R, et al.
1051 Optimizing taxonomic classification of marker-gene amplicon sequences with
1052 QIIME 2’s q2-feature-classifier plugin. *Microbiome.* *Microbiome*; 2018;6:1–17.

1053 51. Quast C, Pruesse E, Yilmaz P, Gerken J, Schweer T, Yarza P, et al. The
1054 SILVA ribosomal RNA gene database project: Improved data processing and
1055 web-based tools. *Nucleic Acids Res.* 2013;41:590–6.

1056 52. Yilmaz P, Parfrey LW, Yarza P, Gerken J, Pruesse E, Quast C, et al. The
1057 SILVA and “all-species Living Tree Project (LTP)” taxonomic frameworks.
1058 *Nucleic Acids Res.* 2014;42:643–8.

1059 53. Price MN, Dehal PS, Arkin AP. FastTree 2 - Approximately maximum-
1060 likelihood trees for large alignments. *PLoS One.* 2010;5.

1061 54. Lozupone C, Knight R. UniFrac: A new phylogenetic method for comparing
1062 microbial communities. *Appl Environ Microbiol.* 2005;71:8228–35.

1063 55. Anderson MJ, Walsh DCI. PERMANOVA , ANOSIM , and the Mantel test
1064 in the face of heterogeneous dispersions : What null hypothesis are you testing ?
1065 *Ecol Monogr.* 2013;83:557–74.

- 1066 56. Clarke KR, Ainsworth M. A method of linking multivariate community
1067 structure to environmental variables. *Mar Ecol Prog Ser.* 1993;92:205–19.
- 1068 57. Spearman C. The Proof and Measurement of Association between Two
1069 Things. *Am J Psychol.* 1904;15:72–101.
- 1070 58. Gonzalez A, Navas-Molina JA, Kosciulek T, McDonald D, Vázquez-Baeza
1071 Y, Ackermann G, et al. Qiita: rapid, web-enabled microbiome meta-analysis.
1072 *Nat Methods [Internet]. Springer US;* 2018;15:796–8. Available from:
1073 <http://dx.doi.org/10.1038/s41592-018-0141-9>
- 1074 59. Bokulich NA, Dillon MR, Zhang Y, Rideout R, Bolyen E, Li H, et al. q2-
1075 longitudinal : Longitudinal and Paired-Sample Analyses of Microbiome Data.
1076 *mSystems.* 2018;3:1–9.
- 1077 60. Bokulich NA, Dillon M, Bolyen E, Kaehler BD, Huttley GA, Caporaso JG.
1078 q2-sample-classifier: machine-learning tools for microbiome classification and
1079 regression. *J Open Source Softw.* 2018;3:934.
- 1080 61. Morton JT, Sanders J, Quinn RA, Mcdonald D, Gonzalez A, Vázquez-Baeza
1081 Y, et al. Balance Trees Reveal Microbial Niche Differentiation. *mSystems.*
1082 2017;2:1–11.
- 1083 62. Mandal S, Van Treuren W, White RA, Eggesbø M, Knight R, Peddada SD.
1084 Analysis of Composition of Microbiomes (ANCOM): A novel method for
1085 studying microbial composition. *Microb Ecol Health Dis.* 2015;26:27663.
- 1086 63. Fernandes AD, Macklaim JM, Linn TG, Reid G, Gloor GB. ANOVA-Like
1087 Differential Expression (ALDEx) Analysis for Mixed Population RNA-Seq.
1088 *PLoS One.* 2013;8.
- 1089 64. Morton JT, Marotz C, Washburne A, Silverman J, Zaramela LS, Edlund A,
1090 et al. Establishing microbial composition measurement standards with reference

1091 frames. *Nat Commun* [Internet]. Springer US; 2019;10. Available from:
1092 <http://dx.doi.org/10.1038/s41467-019-10656-5>

1093 65. Martino C, Morton J, Marotz C, Thompson L, Tripathi A, Knight R, et al. A
1094 novel sparse compositional technique reveals microbial perturbations.
1095 *mSystems* [Internet]. 2019;4:1–13. Available from:
1096 <https://msystems.asm.org/content/msys/4/1/e00016-19.full.pdf>

1097 66. Fedarko MW, Martino C, Morton JT, González A, Rahman G, Marotz CA,
1098 et al. Visualizing 'omic feature rankings and log-ratios using Qurro. *NAR*
1099 *Genomics Bioinforma.* 2020;2:1–7.

1100 67. Knights D, Kuczynski J, Charlson ES, Zaneveld J, Mozer MC, Collman RG,
1101 et al. Bayesian community- wide culture-independent microbial source tracking.
1102 2011;8:6–10.

1103 68. Langille MGI, Zaneveld J, Caporaso JG, McDonald D, Knights D, Reyes J
1104 a, et al. Predictive functional profiling of microbial communities using 16S
1105 rRNA marker gene sequences. *Nat Biotechnol* [Internet]. Nature Publishing
1106 Group; 2013;31:814–21. Available from: <http://dx.doi.org/10.1038/nbt.2676>

1107 69. Markowitz VM, Chen I-MA, Chu K, Szeto E, Palaniappan K, Pillay M, et
1108 al. IMG/M 4 version of the integrated metagenome comparative analysis
1109 system. *Nucleic Acids Res* [Internet]. 2014;42:D568–73. Available from:
1110 <http://nar.oxfordjournals.org/lookup/doi/10.1093/nar/gkt919>

1111 70. Ward T, Larson J, Meulemans J, Hillmann B, Lynch J, Sidiropoulos D, et al.
1112 BugBase Predicts Organism Level Microbiome Phenotypes. *bioRxiv.* 2017;1–
1113 19.

1114 71. Wattam AR, Abraham D, Dalay O, Disz TL, Driscoll T, Gabbard JL, et al.
1115 PATRIC, the bacterial bioinformatics database and analysis resource. *Nucleic*

- 1116 Acids Res. 2014;42:581–91.
- 1117 72. R Core Team. R: A Language and Environment for Statistical Computing
1118 [Internet]. Team RDC, editor. R Found. Stat. Comput. Vienna, Austria: R
1119 Foundation for Statistical Computing; 2014. Available from: [http://www.r-](http://www.r-project.org)
1120 [project.org](http://www.r-project.org)
- 1121 73. Nadkarni MA, Martin FE, Jacques NA, Hunter N. Determination of
1122 bacterial load by real-time PCR using a broad-range (universal) probe and
1123 primers set. *Microbiology*. 2002;148:257–66.
- 1124 74. Hultman J, Tamminen M, Pärnänen K, Cairns J, Karkman A, Virta M. Host
1125 range of antibiotic resistance genes in wastewater treatment plant influent and
1126 effluent. *FEMS Microbiol Ecol*. 2018;94:1–10.
- 1127 75. Muziasari WI, Managaki S, Pärnänen K, Karkman A, Lyra C, Tamminen M,
1128 et al. Sulphonamide and trimethoprim resistance genes persist in sediments at
1129 Baltic Sea aquaculture farms but are not detected in the surrounding
1130 environment. *PLoS One*. 2014;9:1–7.
- 1131 76. Eckert C, Gautier V, Arlet G. DNA sequence analysis of the genetic
1132 environment of various blaCTX-M genes. *J Antimicrob Chemother*.
1133 2006;57:14–23.
- 1134 77. Tamminen M, Karkman A, Lõhmus A, Muziasari WI, Takasu H, Wada S, et
1135 al. Tetracycline resistance genes persist at aquaculture farms in the absence of
1136 selection pressure. *Environ Sci Technol*. 2011;45:386–91.
- 1137 78. Scholz CFP, Kilian M. The natural history of cutaneous propionibacteria,
1138 and reclassification of selected species within the genus propionibacterium to
1139 the proposed novel genera acidipropionibacterium gen. Nov., cutibacterium gen.
1140 nov. and pseudopropionibacterium gen. nov. *Int J Syst Evol Microbiol*.

- 1141 2016;66:4422–32.
- 1142 79. Heinicke C, Verseux C. Surface operations during a long-duration mars
1143 simulation mission. *Proc Int Astronaut Congr IAC*. 2017;8:5459–64.
- 1144 80. Lax S, Smith DP, Hampton-Marcell J, Owens SM, Handley KM, Scott NM,
1145 et al. Longitudinal analysis of microbial interaction between humans and the
1146 indoor environment. *Science* (80-) [Internet]. 2014 [cited 2014 Aug
1147 28];345:1048–52. Available from:
1148 <http://www.sciencemag.org/cgi/doi/10.1126/science.1254529>
- 1149 81. Sharma A, Richardson M, Cralle L, Stamper CE, Maestre JP, Stearns-Yoder
1150 KA, et al. Longitudinal homogenization of the microbiome between both
1151 occupants and the built environment in a cohort of United States Air Force
1152 Cadets. *Microbiome*. *Microbiome*; 2019;7:1–17.
- 1153 82. Chase J, Fouquier J, Zare M, Sonderegger DL, Knight R, Kelley ST, et al.
1154 Geography and Location Are the Primary Drivers of Office Microbiome
1155 Composition. *mSystems*. 2016;1:1–18.
- 1156 83. McDonald D, Hyde ER, Debelius JW, Morton JT, Gonzalez A, Ackermann
1157 G, et al. American Gut: an Open Platform for Citizen-Science Microbiome
1158 Research. *mSystems* [Internet]. 2018;3:277970. Available from:
1159 <http://msystems.asm.org/content/msys/3/3/e00031-18.full.pdf>
- 1160 84. Adams RI, Bateman AC, Bik HM, Meadow JF. Microbiota of the indoor
1161 environment: a meta-analysis. *Microbiome* [Internet]. BioMed Central Ltd;
1162 2015 [cited 2015 Oct 15];3:49. Available from:
1163 <http://www.microbiomejournal.com/content/3/1/49/abstract>
- 1164 85. Adams RI, Bhangar S, Pasut W, Arens EA, Taylor JW, Lindow SE, et al.
1165 Chamber bioaerosol study: Outdoor air and human occupants as sources of

- 1166 indoor airborne microbes. PLoS One [Internet]. 2015;10:1–18. Available from:
1167 <http://dx.doi.org/10.1371/journal.pone.0128022>
- 1168 86. Hospodsky D, Qian J, Nazaroff WW, Yamamoto N, Bibby K, Rismani-
1169 Yazdi H, et al. Human occupancy as a source of indoor airborne bacteria. PLoS
1170 One [Internet]. 2012 [cited 2014 Jan 22];7:e34867. Available from:
1171 <http://www.pubmedcentral.nih.gov/articlerender.fcgi?artid=3329548&tool=pmc>
1172 [entrez&rendertype=abstract](http://www.pubmedcentral.nih.gov/articlerender.fcgi?artid=3329548&tool=pmc&rendertype=abstract)
- 1173 87. Gilbert JA, Stephens B. Microbiology of the built environment. Nat Rev
1174 Microbiol [Internet]. Springer US; 2018;16:661–70. Available from:
1175 <http://dx.doi.org/10.1038/s41579-018-0065-5>
- 1176 88. Stephens B. What Have We Learned about the Microbiomes of Indoor
1177 Environments? mSystems [Internet]. 2016;1:e00083-16. Available from:
1178 <http://msystems.asm.org/lookup/doi/10.1128/mSystems.00083-16>
- 1179 89. Voorhies AA, Mark Ott C, Mehta S, Pierson DL, Crucian BE, Feiveson A,
1180 et al. Study of the impact of long-duration space missions at the International
1181 Space Station on the astronaut microbiome. Sci Rep [Internet]. Springer US;
1182 2019;9:1–17. Available from: <http://dx.doi.org/10.1038/s41598-019-46303-8>
- 1183 90. Grice EA, Kong HH, Conlan S, Deming CB, Davis J, Young AC, et al.
1184 Topographical and Temporal Diversity of the Human Skin Microbiome.
1185 Science (80-) [Internet]. 2009;324:1190–2. Available from:
1186 <http://www.sciencemag.org/cgi/doi/10.1126/science.1171700>
- 1187 91. Grice EA, Segre JA. The skin microbiome. Nat Rev Microbiol [Internet].
1188 Nature Publishing Group; 2011;9:244–53. Available from:
1189 <http://dx.doi.org/10.1038/nrmicro2537>
- 1190 92. Morris BEL, Henneberger R, Huber H, Moissl-Eichinger C. Microbial

- 1191 syntrophy: Interaction for the common good. *FEMS Microbiol Rev.*
1192 2013;37:384–406.
- 1193 93. Flores GE, Caporaso JG, Henley JB, Rideout JR, Domogala D, Chase J, et
1194 al. Temporal variability is a personalized feature of the human microbiome.
1195 *Genome Biol* [Internet]. 2014 [cited 2014 Dec 3];15:531. Available from:
1196 file:///C:/Users/hl/Documents/Word Files/Sloan Fdn 2010/Diversity/Flores et al
1197 2014 Genome Biology-Temporal variability is a personalized feature of the
1198 human microbiome.pdf
- 1199 94. Meadow JF, Altrichter AE, Bateman AC, Stenson J, Brown G, Green JL, et
1200 al. Humans differ in their personal microbial cloud. *PeerJ* [Internet].
1201 2015;3:e1258. Available from: <https://peerj.com/articles/1258>
- 1202 95. Franzosa EA, Huang K, Meadow JF, Gevers D, Lemon KP, Bohannan BJM,
1203 et al. Identifying personal microbiomes using metagenomic codes. *Proc Natl*
1204 *Acad Sci U S A.* 2015;112:E2930–8.
- 1205 96. Leung MHY, Tong X, Wilkins D, Cheung HHL, Lee PKH. Individual and
1206 household attributes influence the dynamics of the personal skin microbiota and
1207 its association network. *Microbiome.* *Microbiome*; 2018;6:16–21.
- 1208 97. Song SJ, Lauber C, Costello EK, Lozupone CA, Humphrey G, Berg-lyons
1209 D, et al. Cohabiting family members share microbiota with one another and
1210 with their dogs. *Elife.* 2013;1–22.
- 1211 98. Fyhrquist N, Ruokolainen L, Suomalainen A, Lehtimäki S, Veckman V,
1212 Vendelin J, et al. *Acinetobacter* species in the skin microbiota protect against
1213 allergic sensitization and inflammation. *J Allergy Clin Immunol.*
1214 2014;134:1301-1309.e11.
- 1215 99. Bashir M, Ahmed M, Weinmaier T, Ciobanu D, Ivanova N, Pieber TR, et al.

- 1216 Functional Metagenomics of Spacecraft Assembly Cleanrooms : Presence of
1217 Virulence Factors Associated with Human Pathogens. *Front Microbiol.*
1218 2016;7:1–12.
- 1219 100. Lax S, Sangwan N, Smith D, Larsen P, Handley KM, Richardson M, et al.
1220 Bacterial colonization and succession in a newly opened hospital. *Sci Transl*
1221 *Med* [Internet]. 2017;9:1–11. Available from:
1222 <http://stm.sciencemag.org/content/9/391/eaah6500>
- 1223 101. Mahnert A, Moissl-Eichinger C, Zojer M, Bogumil D, Mizrahi I, Rattei T,
1224 et al. Man-made microbial resistances in built environments. *Nat Commun*
1225 [Internet]. Springer US; 2019;9:68. Available from:
1226 <http://dx.doi.org/10.1038/s41467-019-08864-0>
- 1227 102. Mogul R, Barding GA, Lalla S, Lee S, Madrid S, Baki R, et al. Metabolism
1228 and Biodegradation of Spacecraft Cleaning Reagents by Strains of Spacecraft-
1229 Associated *Acinetobacter*. *Astrobiology*. 2018;18:1517–27.
- 1230 103. Hendrickx L, Wever H De, Hermans V, Mastroleo F, Morin N. Microbial
1231 ecology of the closed artificial ecosystem MELiSSA (Micro-Ecological Life
1232 Support System Alternative): Reinventing and compartmentalizing the Earth ' s
1233 food and oxygen regeneration system for long-haul space exploration missions.
1234 *Res Microbiol*. 2006;157:77–86.
- 1235 104. Abeles SR, Jones MB, Santiago-Rodriguez TM, Ly M, Klitgord N,
1236 Yooseph S, et al. Microbial diversity in individuals and their household contacts
1237 following typical antibiotic courses. *Microbiome* [Internet]. *Microbiome*;
1238 2016;4:1–12. Available from: <http://dx.doi.org/10.1186/s40168-016-0187-9>
- 1239 105. Turrone S, Rampelli S, Biagi E, Consolandi C, Severgnini M, Peano C, et
1240 al. Temporal dynamics of the gut microbiota in people sharing a confined
1241 environment, a 520-day ground-based space simulation, MARS500.

1242 Microbiome [Internet]. Microbiome; 2017;5:39. Available from:
1243 [http://microbiomejournal.biomedcentral.com/articles/10.1186/s40168-017-](http://microbiomejournal.biomedcentral.com/articles/10.1186/s40168-017-0256-8)
1244 [0256-8](http://microbiomejournal.biomedcentral.com/articles/10.1186/s40168-017-0256-8)

1245 106. Avila-Herrera A, Thissen J, Urbaniak C, Be NA, Smith DJ, Karouia F, et
1246 al. Crewmember microbiome may influence microbial composition of ISS
1247 habitable surfaces. PLoS One [Internet]. 2020;15:1–20. Available from:
1248 <http://dx.doi.org/10.1371/journal.pone.0231838>

1249

1250

1251 **Figure and Table legend**

1252 **Fig. 1: Microbiome profile of crew and built environment samples, all time points**
1253 **included.** A to C: violin plots (kernel probability density of Shannon values, displaying the
1254 alpha diversity) including individual data points and a box with median and interquartile range.
1255 A: Sampled surface types: skin of crew and locations of the built environment. B: Built
1256 environment surfaces: BR (desk in bedroom), KC (kitchen floor), MR (desk in main room),
1257 TB (toilet bowl). C: Samples from the individual crew members (A-F). D: Linear discriminant
1258 analysis effect size (LEfSe) on samples from crew and built environment. E: LEfSe on samples
1259 from built environment surfaces. F: LEfSe on samples from individual crew members. G to H:
1260 Beta diversity represented by PCoA plots based on weighted UniFrac metrics and a rarefaction
1261 depth of 3,000 ASVs per sample. G: Microbial profile of samples from built environment and
1262 crew. H: Microbial profile of the individual crew members and sampling locations of the built
1263 environment.

1264 **Fig. 2: Longitudinal development of diversity and composition.** A: Volatility analysis of
1265 Shannon diversity resolved to sample type (built environment and human skin). B: Volatility
1266 analysis of Shannon diversity resolved to individual crew members and sampled locations
1267 within the HI-SEAS habitat. C: Meta volatility analysis of longitudinal microbial diversity of
1268 samples taken within the HI-SEAS habitat and inside other built environments. D: Volatility
1269 analysis along PCoA Axis 1 showing weighted UniFrac distances for different sample types
1270 (built environment and human skin). E: Volatility analysis along PCoA Axis 1 showing
1271 weighted UniFrac distances for individual crew members and sampled locations within the HI-
1272 SEAS habitat.

1273 **Fig. 3. Microbial dynamics in distinct phases and for representative features.** A:
1274 Proportion plots of differential feature abundances using balances in gneiss on genus level
1275 grouped into four distinct phases. Numerators are colored in light blue, denominators in dark
1276 blue. B: Volatility analysis based on linear regression models with time of *Acinetobacter*,
1277 *Staphylococcus* and *Methanobrevibacter sp.*

1278 **Fig. 4 Source tracking of microbial signatures** according to SourceTracker2. Panels A to F
1279 show respective crew members A to F as a sink of microbial dispersal.

1280 **Fig. 5. Linear regression with time of predicted phenotypes from BugBase** shown as
1281 volatility plots (sorted according to regression with time).

1282 **Fig. 6. Overall bacterial load and abundance of selected antimicrobial resistances.** A:
1283 Volatility analysis of bacterial 16S rRNA gene copies per m² according to qPCR. B: Linear
1284 regression volatility analysis of selected resistance gene copies per m² according to qPCR.